Published by Institute of Physics Publishing for SISSA

Received: *January 21, 2008*
Revised: *February 8, 2008*
Accepted: *April 13, 2008*
Published: *April 29, 2008*

The fine-tuning price of neutralino dark matter in models with non-universal Higgs masses

John Ellis

Theory Division, Physics department, CERN, CH-1211 Geneve 23, Switzerland
E-mail: John.Ellis@cern.ch

S.F. King

School of Physics and Astronomy, University of Southampton, Southampton, SO17 1BJ, U.K.
E-mail: sfk@hep.phys.soton.ac.uk

J.P. Roberts

Institute of Theoretical Physics, Warsaw University, Hoza 69, 00-681, Warsaw, Poland
E-mail: roberts@fuw.edu.pl

Abstract: We study the amounts of fine-tuning of the parameters of the MSSM with non-universal soft supersymmetry-breaking contributions to the Higgs masses (the NUHM) that would be required for the relic neutralino density to lie within the range favoured by WMAP and other astrophysical and cosmological observations. Such dark matter fine-tuning is analogous to the commonly studied electroweak fine-tuning associated with satisfying the electroweak symmetry breaking conditions, which we also study for completeness. We identify several distinct regions of the NUHM parameter space: a bulk region, a $\tilde{\tau} - \tilde{\chi}_1^0$ coannihilation region, a pseudoscalar Higgs funnel region, a focus-point bino/higgsino region and a $\tilde{\nu} - \tilde{\chi}_1^0$ coannihilation region. Within each region, we analyse specific representative points for which we provide breakdowns of the contributions to the dark matter fine-tuning associated with the different NUHM parameters. In general, the NUHM offers points with both smaller and larger amounts of dark matter fine-tuning than points in the corresponding regions of the CMSSM. Lower amounts of dark matter fine-tuning typically arise at points where several different (co)annihilation processes contribute, e.g., at junctions between regions with different dominant processes. We comment on the prospects for using collider measurements to estimate the likely dark matter density within the NUHM framework.

Keywords: Supersymmetry Phenomenology, Cosmology of Theories beyond the SM.

JHEP04(2008)099

Contents

JHEP04(2008)099

1. Introduction

The primary utilitarian motivation for supersymmetry being accessible to experiments at the electroweak scale, e.g., at the LHC, depends on its ability to alleviate the problem of fine-tuning of electroweak symmetry breaking present in the Standard Model [1, 2]. A supplementary phenomenological motivation for weak-scale supersymmetry is its ability to provide the cold dark matter required by astrophysics and cosmology [3, 4]. This is a natural feature of supersymmetric models that conserve R parity, with the lightest neutralino $\tilde{\chi}_1^0$ being particularly well-suited to provide the preferred amount of cold dark matter if it is the lightest supersymmetric particle (LSP) and weighs less than about 1 TeV [3, 5]. Within the general supersymmetric framework, one may find more plausible regions of the supersymmetric parameter space that are less fine-tuned, in the sense that the values of the model parameters chosen at some high input scale require less delicate adjustment in order to obtain the correct value of the electroweak scale [1, 6], as measured by M_Z, or the correct value of the cold dark matter density $\Omega_{\rm CDM}h^2$ [7 – 10].

It is hard to make this type of plausibility argument at all rigorous: it is notoriously difficult to make probabilistic statements about the unique (by definition) Universe in

which we live, it is largely a matter of personal choice which derived quantity one should consider and which input parameters one wishes to avoid fine-tuning, it is difficult to argue conclusively for the superiority of one measure of fine-tuning over any other, and even less easy to agree on a 'pain threshold' in the amount of fine-tuning one is prepared to tolerate [6]. Nevertheless, within a given model framework with its specific input parameters, it is legitimate to consider some important derived quantity such as $\Omega_{\rm CDM}h^2$, and compare the amounts of fine-tuning required in different regions of its parameter space, which frequently do not depend very sensitively on the specific sensitivity measure employed.

Moreover, even if one does not accept that the less sensitive parameter regions are more plausible, measuring the dark matter fine-tuning may have other uses. For example, one hopes (expects) some day to discover supersymmetry and start to measure the values of its parameters. Unavoidably, these will have non-negligible measurement errors, and these uncertainties propagate via the dark matter fine-tuning parameters into the calculation, e.g., of $\Omega_{\rm CDM}h^2$. One of the key features of supersymmetry is its ability to provide a calculable amount of cold dark matter, and it is interesting to know how accurately which of its parameters must be measured in order to calculate $\Omega_{\rm CDM}h^2$ with an accuracy comparable to that quoted by astrophysicists and cosmologists [7, 11]. An accurate calculation of $\Omega_{\rm CDM}h^2$ might also reveal some deficiency of the supersymmetric explanation of the cold dark matter, and possibly the need for some other new physics in addition.

It is important to note that the parameters we refer to here are the GUT-scale soft supersymmetry-breaking masses and couplings, whereas experiments would measure directly physical masses and mixings at much lower energies. Ideally, one would calculate the relic density directly from the low-energy measurements of MSSM parameters. However it will be difficult, if not impossible, to pin down all the key parameters using LHC data alone, except by making supplementary assumptions about the pattern of supersymmetry breaking at the GUT scale, as we do here. Assuming a structure of GUT-scale unification, one may use experimental measurements to constrain these fewer high-energy parameters. The strength of the constraints will depend on the magnitudes of these parameters and the experimental tools available. Very likely some accelerator beyond the LHC will be needed, but we do not yet know what will be available. The fine-tuning measures we calculate here show clearly which of the high-energy parameters are most important for a precise calculation of the relic density, and hence contribute to the 'wish list' for such an accelerator.

For these reasons, we make no further apologies for considering the fine-tuning of $\Omega_{\rm CDM}h^2$ in this paper, which we shall refer to as "dark matter fine-tuning" [7 – 10] to distinguish it from the more commonly studied "electroweak fine-tuning" [1, 6], which we also consider for completeness. The issue of dark matter fine-tuning has been considered previously in the context of several different models including the constrained minimal supersymmetric extension of the Standard model (CMSSM) [7], in which the soft supersymmetry-breaking scalar masses m_0, gaugino masses $m_{1/2}$ and trilinear parameters A_0 are each assumed to be universal, a more general MSSM with non-universal third family scalars and gaugino masses [8], a string-inspired non-universal model [9] and SUSY GUTs with non-universal gaugino masses [10]. Here we extend such considerations to

JHEP04(2008)099

models with non-universal soft supersymmetry-breaking contributions to the Higgs masses (NUHM). Within this NUHM framework, the independent input parameters may be taken as [12 – 14]

$$a_{\rm NUHM} = \left\{ m_0,\ m_{H_1},\ m_{H_2},\ m_{1/2},\ A_0,\ \tan\beta,\ {\rm sign}(\mu) \right\}, \tag{1.1}$$

and we take as our measure of dark matter fine-tuning the quantity

$$\Delta_\Omega \ \equiv \ {\rm Max}_i \left| \frac{a_i}{\Omega_\chi} \frac{\partial \Omega_\chi}{\partial a_i} \right|. \tag{1.2}$$

Our objective will be three-fold: to compare the amount of dark matter fine-tuning required within the NUHM to that required within the CMSSM, to identify the regions of the NUHM parameter space that require relatively less (or more) dark matter fine-tuning, and thereby to quantify the accuracy in the determination of the GUT-scale NUHM parameters that would be needed in order to calculate $\Omega_\chi h^2$ with any desired accuracy.

The regions of the NUHM parameter space where $\Omega_\chi h^2$ falls within the range favoured by WMAP and other experiments has been studied quite extensively, for example in [14]. It shares several features in common with the more restrictive CMSSM framework proposed in [15] and extensively studied in [16]. For example, there are regions where $\tilde{\chi}_1^0$ - stau coannihilation is important, and others where $\tilde{\chi}_1^0$ pairs annihilate rapidly via direct-channel H, A poles. However, other possibilities also occur. For example, there are regions where $\tilde{\chi}_1^0$ - sneutrino coannihilation is dominant. Also there are regions where rapid-annihilation and bulk regions, which are normally separated by a coannihilation strip, approach each other and may even merge. As we discuss below in more detail, the sneutrino coannihilation regions exhibit relatively high dark matter fine-tuning, whereas the 'merger' regions may require significantly less dark matter fine-tuning.

In this work we provide a first calculation of the dark matter fine-tuning for the regions of the NUHM that are favoured by dark matter measurements. In addition, we present a first calculation of the electroweak fine-tuning within this model and update the parameter scans for the current measurement of the top mass.

The rest of the paper is laid out as follows. In section 2 we summarise the methods used in our numerical studies. Next, in section 3 we review the familiar case of the CMSSM, which serves as a baseline for later comparison. Then, in section 4 we study dark matter within the NUHM model in which universality between the soft supersymmetry-breaking masses of the sfermions (squarks and sleptons) and Higgs multiplets is broken. Finally, in section 5 we present our conclusions.

2. Methodology

2.1 Codes

In order to study the low-energy phenomenology of the NUHM, we need a tool to run the mass spectrum from the GUT scale down to the electroweak scale using the renormalisation group equations (RGEs) [17]. For this purpose we use the RGE code `SoftSusy` [18]. This interfaces with the MSSM package within `micrOMEGAs` [19], which we use to calculate

JHEP04(2008)099

the dark matter relic density $\Omega_{\rm CDM}h^2$, $BR(b \to s\gamma)$ and δa_μ. We take $m_t = 170.9\,\text{GeV}$ throughout.

2.2 Theoretical, experimental and cosmological bounds

After running the mass spectrum of any chosen model parameter set from the GUT scale down to the electroweak scale, we perform a number of checks on the phenomenological acceptability of the point chosen. A point is ruled out if:

1. It does not provide radiative electroweak symmetry breaking (REWSB). Such regions are displayed in light red in the subsequent figures.

2. It violates the bounds on particle masses provided by the Tevatron and LEP 2. Such regions are displayed in light blue.[1]

3. It results in a lightest supersymmetric particle (LSP) that is not the lightest neutralino. We colour these regions light green.

In the remaining parameter space we display the 1- and 2-σ regions for δa_μ and $BR(b \to s\gamma)$, as well as plotting the 2-σ region for the relic density allowed by WMAP and other observations.

2.2.1 δa_μ

Present measurements of the anomalous magnetic moment of the muon a_μ deviate from theoretical calculations of the SM contribution based on low-energy e^+e^- data.[2] Taking the current experimental world average and the state-of-the-art SM value from [21], there is a discrepancy:

$$(a_\mu)_{\rm exp} - (a_\mu)_{\rm SM} = \delta a_\mu = (2.95 \pm 0.88) \times 10^{-9}, \tag{2.1}$$

which amounts to a 3.4-σ deviation from the SM value. As already mentioned, we use `micrOMEGAs` to calculate the SUSY contribution to $(g-2)_\mu$. The dominant theoretical errors in this calculation are in the SM contribution, so in our analysis we neglect the theoretical error in the calculation of the SUSY contribution.

2.2.2 $BR(b \to s\gamma)$

The variation of $BR(b \to s\gamma)$ from the value predicted by the Standard Model is highly sensitive to SUSY contributions arising from charged Higgs-top loops and chargino-stop loops. To date no deviation from the Standard Model has been detected. We take the

[1] The current LEP 2 bound on the lightest MSSM Higgs stands at 114.4 GeV. However, there is a theoretical uncertainty of some 3 GeV in the determination of the mass of the light Higgs [20]. Rather than placing a hard cut on the parameter space for the Higgs mass, instead we plot a line at $m_h = 111\,\text{GeV}$ and colour the region in which $m_h < 111\,\text{GeV}$ in very light grey-blue.

[2] There is a long-running debate whether the calculation of the hadronic vacuum polarisation in the Standard Model should be done with e^+e^- data, or with τ decay data. The weight of evidence indicates the e^+e^- estimate is more reliable so we use the e^+e^- value in our work.

JHEP04(2008)099

current world average from [22], based on the BELLE [23], CLEO [24] and BaBar [25] measurements:

$$BR(b \to s\gamma) = (3.55 \pm 0.26) \times 10^{-4}. \tag{2.2}$$

Again, we use `micrOMEGAs` to calculate both the SM value of $BR(b \to s\gamma)$ and the SUSY contributions. It is hard to estimate the theoretical uncertainty in the calculation of the SUSY contributions, but note that there is an uncertainty of 10% in the NLO SM prediction of $BR(b \to s\gamma)$ [26].[3] As with δa_μ, we plot the 1-σ and 2-σ experimental ranges, and do not include a theoretical error in the calculation.

2.2.3 $\Omega_{\rm CDM}h^2$

Evidence from the cosmic microwave background, the rotation curves of galaxies and other astrophysical data point to a large amount of cold non-baryonic dark matter in the universe. The present measurements [28] indicate the following value for the current cold dark matter density:

$$\Omega_{\rm CDM}h^2 = 0.106 \pm 0.008. \tag{2.3}$$

We calculate the relic dark matter density with `micrOMEGAs` using the *fast* approximation. Given a low-energy mass spectrum, `micrOMEGAs` gives an estimated precision of 1% in the theoretical prediction of the relic density. This is negligible compared to the present observational error, so the 2-σ band plotted takes into account only the experimental error.[4]

In the following sections, we calculate the dark-matter fine-tuning for any point that lies within the 2σ allowed region, and indicate the amount using colour coding. We also display electroweak fine-tuning contours over the different regions.

3. The constrained minimal supersymmetric standard model

We first review the familiar Constrained Minimal Supersymmetric Standard Model (CMSSM) [15, 16]. which serves as a standard to which we compare the parameter space of the NUHM.

The CMSSM has a much simpler spectrum of soft masses than the full MSSM. First, all of the soft squark and slepton (mass)^2 matrices are chosen to be diagonal and universal at the GUT scale with the diagonal entries equal to m_0^2. Secondly both the soft Higgs

[3] We recall that `micrOMEGAs` calculates the SM contribution to $BR(b \to s\gamma)$ to NLO. A first estimate of the SM prediction of $BR(b \to s\gamma)$ to NNLO was presented in [27]. This showed a decrease of around 0.4×10^{-4} in the central value of the SM prediction. The implementation of the NNLO contributions in the calculation is non-trivial and its implementation in `micrOMEGAs` is currently underway. As a result we do not include this decrease in the results we present, but instead note that *positive* SUSY contributions to $BR(b \to s\gamma)$ look likely to be favoured in future. This would favour a negative sign of μ and thus cause tension with $(g-2)_\mu$.

[4] We emphasize that the quoted 1% accuracy is for a given low-energy spectrum, which is obtained using `softsusy`. However, there are differences in the details of the mass spectrum between codes [29], for given high-energy inputs, and different dark matter regions have different levels of sensitivity to these variations: see [30] for a detailed study. The result of the discrepancies between codes is to move the dark matter regions slightly in the GUT scale parameter space. As we are interested in broad features of these regions, rather than their precise locations, these uncertainties are not important for our purposes.

JHEP04(2008)099

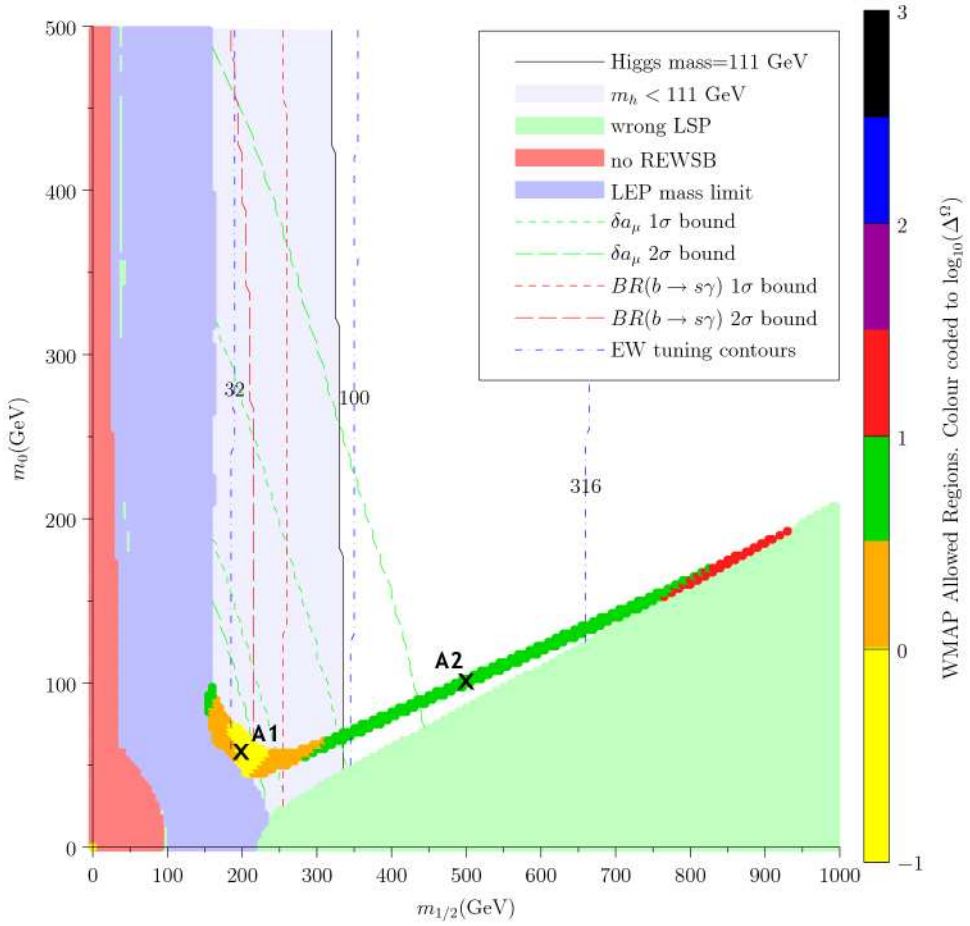

Figure 1: The $(m_{1/2}, m_0)$ plane of the CMSSM with $A_0 = 0$, $\tan\beta = 10$ and sign(μ) +ve.

(mass)^2 are also set equal to m_0^2. Additionally, all the gaugino masses are assumed to be unified with a value $m_{1/2}$ at the GUT scale. Finally, we take the trilinear coupling matrices to have only one non-zero entry (the third-family dominance approximation) and assume that all these entries are equal to a common value A_0. Requiring that electroweak symmetry be broken radiatively to give the observed electroweak boson masses, we trade the soft parameters μ and B for $\tan\beta$, the ratio of the Higgs vevs, and the sign of μ. This results in a model with four free parameters and a sign:

$$a_{\text{CMSSM}} \in \left\{m_0,\ m_{1/2},\ A_0,\ \tan\beta,\ \text{sign}(\mu)\right\}. \tag{3.1}$$

Although our main focus is the dark-matter fine-tuning, we also report the required amounts of electroweak fine-tuning for specific cases of interest.

In figure 1 we show the $(m_0, m_{1/2})$ plane of the CMSSM for $A_0 = 0$, $\tan\beta = 10$ and sign(μ) positive. At low m_0 the parameter space is ruled out because $m_{\tilde{\tau}} < m_{\tilde{\chi}_1^0}$, resulting in a stau LSP (light green). Regions at low $m_{1/2}$ are ruled out by LEP 2 bounds on the masses of the charginos and sleptons (light blue). A larger range of m_0 is ruled out by

JHEP04(2008)099

Parameter	A1		A2	
	value	Δ^Ω	value	Δ^Ω
m_0	60	0.62	100	5.7
$m_{1/2}$	200	0.99	500	5.8
$\tan\beta$	10	0.13	10	1.5
Δ_Ω		0.99		5.8
$\Delta_{\rm EW}$		37		190

Table 1: A summary of the properties of points A1 and A2, shown in figure 1, chosen as representatives of the bulk region (A1) and stau-coannihilation region (A2). We also present a breakdown of the dark-matter and electroweak fine-tunings with respect to each parameter of the CMSSM, except for A_0, which we fix: $A_0 = 0$ here and elsewhere in this paper.

the absence of a light Higgs boson, and we shade the region with $m_h < 111\,\text{GeV}$ (light grey with a black boundary). Finally, the model fits the current δa_μ measurement for low m_0 and $m_{1/2}$. The 1σ and 2σ bounds are shown as a short and long-dashed green lines respectively. At larger m_0 and $m_{1/2}$, the SUSY contribution becomes small as the sparticles that contribute in loops become heavy. Therefore $\delta a_\mu \neq 0$ favours relatively light soft masses.

In the remainder of the parameter space we find the regions that fit the WMAP strip at 2σ, and for each such point we calculate the fine-tuning of the dark matter density. Each point is then plotted with a colour that corresponds to the value of the tuning via the log-scale on the right hand side.

There are two distinct regions that fit the WMAP measurement of the relic density. The first region lies at $m_{1/2} \approx 200\,\text{GeV}$, $m_0 \approx 70\,\text{GeV}$ and contains the point A1. This is the bulk region, which is adjacent to the light blue region that is ruled out by the LEP 2 slepton mass constraint. The lightness of the sleptons enhances neutralino annihilation via t-channel slepton exchange to the extent that it allows bino dark matter to fit the WMAP relic density measurement. This process is relatively insensitive to the precise masses of the neutralino and the sleptons. This is reflected in the fact that much of the bulk region is plotted in yellow, signifying $\Delta^\Omega < 1$. From the breakdown of the tunings of point A1 in table 1 it is clear that the tuning is mainly in the parameters $m_{1/2}$ and m_0. The sensitivity to m_0 is to be expected, as t-channel slepton exchange is clearly dependent on the mass of the exchanged particle. This also explains the sensitivity to $m_{1/2}$ since, although the masses of the sleptons are determined by m_0 at the GUT scale, the running to low energies is dominated by $m_{1/2}$. Thus, in this region the masses of the light sleptons are sensitive to both m_0 and $m_{1/2}$. The relic density is also dependent upon the mass of the LSP, in this case (mainly) a bino with a mass determined primarily by $m_{1/2}$. It is therefore apparent why the sensitivity of the bulk regions lies primarily with m_0 and $m_{1/2}$. The fact that no precise cancellations or balancing of parameters is required explains why the tuning is low. However, the bulk region lies inside a light grey region signifying a Higgs with a mass less than 111 GeV. Therefore we do not consider this region further here.

The second region that fits the observed relic density is the band that contains point

JHEP04(2008)099

A2. This band lies alongside the area that is ruled out by a stau LSP (light green). Along the edge of the light green region, the mass of the stau is close to that of the lightest neutralino, resulting in comparable number densities of both particles around the time of freeze-out. Thus many more annihilation channels must be considered, such as the annihilations of $\tilde{\tau} - \tilde{\tau}$ and $\tilde{\tau} - \tilde{\chi}_1^0$ in addition to $\tilde{\chi}_1^0 - \tilde{\chi}_1^0$. This suppresses the number density of SUSY particles and thus reduces the resultant dark matter relic density. The effect of coannihilation depends strongly upon the number density of NLSPs at freeze-out. This is in turn very sensitive to the mass difference between the NLSP and the LSP. Thus, it may at first sight seem surprising that the $\tilde{\tau}$ coannihilation band is plotted here in green and red, corresponding to relatively low dark matter fine-tuning $\Delta^{\Omega} = 3 - 11$. The reason, as discussed in [8], is that in this region the RGE running results in the mass of the right handed $\tilde{\tau}$ and the mass of the lightest neutralino both being dominantly dependent on $m_{1/2}$, with the stau having a smaller secondary dependence on m_0. As a result, their masses vary together as the soft masses are varied, and Δm is remarkably insensitive to m_0 or $m_{1/2}$. This mitigates the normal sensitivity of the coannihilation region. We take the point A2 as a representative point in this band and provide a breakdown of the individual tunings in table 1. The tuning is equally dependent upon m_0 and $m_{1/2}$, as expected.

As well as the dark-matter fine-tuning, for reference we also calculate the fine-tuning required to fit the electroweak boson masses. This calculation is performed across the parameter space using the same measure as we use for the dark matter fine-tuning. We plot the tuning using blue dot-dashed contours in figure 1, and label each contour with their respective values of $\Delta^{\rm EW} = \max(\Delta_a^{\rm EW})$. We also list the value of $\Delta^{\rm EW}$ in the last row of table 1 for both points we consider. The W boson mass is in general the result of a careful balancing act between the soft masses: the larger the soft masses, the more precisely they must cancel to give the W boson mass. Therefore it is unsurprising that the amount of fine-tuning required to obtain the correct electroweak symmetry breaking increases smoothly with the increasing soft masses. The electroweak and dark matter fine-tunings are largely independent.

Other regions in which the CMSSM fits the observed relic density are seen when we consider larger values of $\tan\beta$. In figure 2 we consider a wider range in the $(m_0, m_{1/2})$ plane and take $\tan\beta = 50$.

Low m_0 is once again ruled out because the stau is the LSP (light green). Equally low $m_{1/2}$ and m_0 are ruled out by searches for the lightest Higgs (light grey with a black boundary) or LEP 2 bounds on the chargino and light sleptons (solid light blue). Finally large m_0 and low $m_{1/2}$ are ruled out as they do not give REWSB (light red). We plot the different regions that fit the relic density using the same colour coding for dark-matter fine-tuning as was used in figure 1.

We now distinguish four regions in which the CMSSM can account for the observed relic density of dark matter. The least interesting of these regions is the bulk region, which once again appears at low m_0 and low $m_{1/2}$, but requires a Higgs lighter than current search limits allow. Moving on from the inaccessible bulk region, we again find the coannihilation strip along the side of the region ruled out because the stau is the LSP. In comparison to figure 1, it is thin and broken. This is a sampling artefact, arising because we have

JHEP04(2008)099

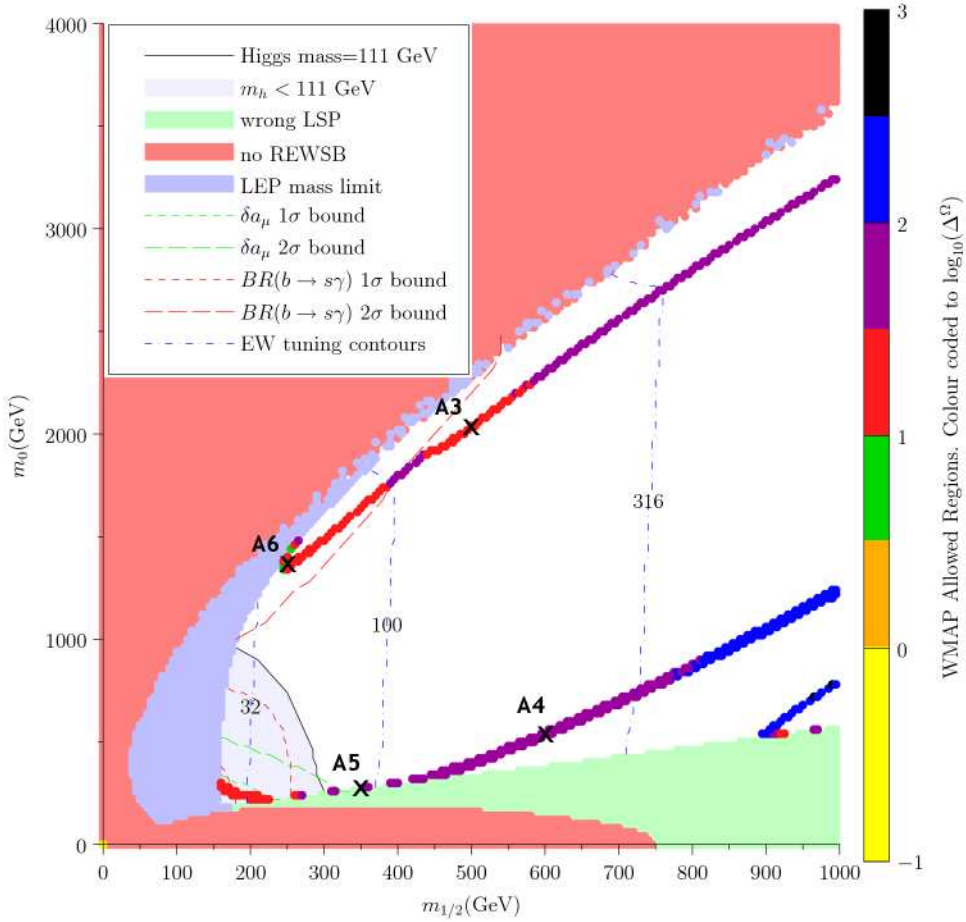

Figure 2: The $(m_0,\ m_{1/2})$ plane of the CMSSM parameter space for $A_0 = 0$, $\tan\beta = 50$ and sign(μ) +ve.

Parameter	A3		A4		A5		A6	
	value	Δ^Ω	value	Δ^Ω	value	Δ^Ω	value	Δ^Ω
m_0	2030	27	540	5.0	277	19	1400	13
$m_{1/2}$	500	18	600	8.0	350	12	250	22
$\tan\beta$	50	2.0	50	76	50	48	50	8.2
Δ_Ω		27		76		48		22
$\Delta_{\rm EW}$		150		230		92		48

Table 2: Here we summarize properties of the points A3-6, shown in figure 2, which represent the higgsino/bino region (A3,6), the pseudoscalar Higgs funnel (A4) and the stau-coannihilation region at large $\tan\beta$ (A5). We also present a breakdown of the dark matter fine-tuning with respect to each parameter, and also list the electroweak fine-tuning.

extended the range of the m_0 scan, and the resolution is not fine enough to resolve the full strip. In contrast to figure 1, here the strip is plotted in purple, designating a dark matter

JHEP04(2008)099

fine-tuning in the range $\Delta^{\Omega} = 30 - 100$.

Consider now the representative point A5 and the corresponding fine-tuning. At large $\tan\beta$, the mass of the $\tilde{\tau}_R$ runs down more than for low $\tan\beta$, and therefore a larger soft mass is necessary to avoid a $\tilde{\tau}$ LSP. For low $\tan\beta$ the $\tilde{\tau}$ coannihilation region occurred when $m_0 \ll m_{1/2}$, whereas here m_0 and $m_{1/2}$ are much closer in magnitude. This reduces the dominance of $m_{1/2}$ in the running and restores the need for a precise balance of m_0 and $m_{1/2}$ to keep the $\tilde{\tau} - \tilde{\chi}_1^0$ mass difference small. However, it is the influence of $\tan\beta$ over the running that dominates the sensitivity.

The second region of interest shows up as two diagonal bands starting beside the light green region ruled out because the stau is the LSP. These lines lie to either side of the line along which $2m_{\tilde{\chi}_1^0} = m_A$, and neutralino annihilation proceeds via the resonant production of a pseudoscalar Higgs boson. This region is known as the pseudoscalar Higgs funnel region. The WMAP lines lie along either side of this resonance, where there is just enough of an enhancement in the annihilation cross section to allow a bino LSP to account for the observed relic density. As a result, the dark matter fine-tuning price of such a region is large. This is reflected in the purple and blue shading of the funnel region, corresponding to a dark matter fine-tuning in the range $\Delta^{\Omega} = 30 - 300$.

We consider the representative point A4 and break down the fine-tuning. The mass of the pseudoscalar Higgs is dependent upon the details of the running of the soft Higgs mass-squared terms, which also determine the Higgs vevs and thus $\tan\beta$. As we require REWSB and set $\tan\beta$ at the start, we can run this chain of logic back the other way. A fixed value of $\tan\beta$ requires a specific value of the soft Higgs mass-squared terms at the low-energy scale. Thus the value of $\tan\beta$ has a significant impact on the pseudoscalar Higgs boson mass. This explains the dominant sensitivity of the pseudoscalar Higgs funnel region to $\tan\beta$. This is to be contrasted with the NUHM, which will allow access to the pseudoscalar Higgs funnel region without large $\tan\beta$, so that naively one might expect a more natural funnel region.

The final WMAP strip lies at large m_0 in all panels. The corner of the parameter space at large m_0 and low $m_{1/2}$ (shown in light red) is ruled out as $\mu^2 < 0$, signifying a failure of REWSB. Along the perimeter of this region $\mu \approx 0$, and μ decreases steadily as one approaches the boundary. As μ decreases, the higgsino component of the LSP increases. Higgsino dark matter annihilates very efficiently resulting in $\Omega_{\rm CDM}h^2 \ll \Omega_{\rm CDM}^{\rm WMAP}h^2$, whereas bino dark matter generally gives $\Omega_{\rm CDM}h^2 \gg \Omega_{\rm CDM}^{\rm WMAP}h^2$. Along the WMAP strip, the higgsino component of the $\tilde{\chi}_1^0$ is large enough that the annihilation cross section is enhanced sufficiently for the relic density to fit the WMAP data. This region is known as the focus-point region. It is sensitive to the composition of the lightest neutralino, and so depends upon the difference between μ and M_1 at the electroweak scale. The region is plotted in red and purple, with a couple of green regions at low $m_{1/2}$. This corresponds to a dark matter fine-tuning of $\Delta^{\Omega} \approx 10$ at low $m_{1/2}$, rising to a dark matter fine-tuning of $\Delta^{\Omega} \approx 60$ at large m_0 and $m_{1/2}$. The kink at $m_{1/2} \approx 450\,GeV$, where the tuning drops (signified by a change from purple to red) corresponds to the top quark mass threshold where processes of the form $\tilde{\chi}_1^0\tilde{\chi}_1^0 \to t\bar{t}$ become kinematically allowed.

We take points A3 and A6 as representative points in this region and break the dark

JHEP04(2008)099

Region	Tuning Range
Pseudoscalar Higgs Funnel	60-1200+
$\tilde{\tau} - \tilde{\chi}_1^0$ coannihilation (large m_0, $m_{1/2}$ or $\tan\beta$)	30-60
$\tilde{\tau} - \tilde{\chi}_1^0$ coannihilation (low m_0, $m_{1/2}$ and $\tan\beta$)	3-10
bino/higgsino region	10-60

Table 3: Here we summarize the DM annihilation channels present within the CMSSM and their associated tunings. This provides a reference to which we will compare the regions accessible within the NUHM.

matter fine-tuning down into its individual elements. At point A3 the LSP is predominantly bino with a small, but significant, higgsino component. The higgsino component is determined by the relative size of $\mu(EW)$ to $M_1(EW)$. As we set $\mu(EW)$ by requiring REWSB, $\mu(EW)$ is determined by the running of the soft Higgs masses. Thus $\mu(EW)$ is sensitive to the soft Higgs mass-squared terms at the GUT scale (set to m_0^2 in the CMSSM). It is also sensitive to strongly-interacting sparticle masses through the RGEs. This once again brings in a sensitivity to m_0, but also to M_3 through its strong influence on the stop quark mass. Therefore $\mu(EW)$ is sensitive to both m_0 and $m_{1/2}$. To achieve the correct balance of bino and higgsino components one needs to balance $\mu(EW)$ and $M_1(EW)$. These both depend strongly upon $m_{1/2}$, with μ also dependent upon m_0. This common dependence on $m_{1/2}$ reduces the dark matter fine-tuning below what one would expect.

At point A6 we consider the kink at the bottom of the higgsino/bino line, where the higgsino and bino components are almost equal. This would normally result in extremely efficient annihilation of neutralinos in the early universe and give $\Omega_{\rm CDM}h^2 \ll \Omega_{\rm CDM}^{\rm WMAP}h^2$. However at this point the neutralino mass is $m_{\tilde{\chi}_1^0} = 79.6\,{\rm GeV}$, disallowing the annihilation of neutralinos to Higgs, Z bosons and $t\bar{t}$. It is also on the W boson threshold, suppressing annihilation to Ws. With these annihilation channels ruled out, the normally efficient annihilation of an LSP with a substantial higgsino fraction is suppressed sufficiently to fit the WMAP relic density. As with point A3, the determining factors for the annihilation cross section are the relative sizes of $\mu(EW)$ and $M_1(EW)$, resulting in a similar pattern and magnitude of dark matter fine-tuning measures.

Once again we also calculate the electroweak fine-tuning across the plane and plot the corresponding contours of $\Delta^{\rm EW}$. As in the case of figure 1, the degree of electroweak tuning increases steadily with increasing $m_{1/2}$. This is because the dominant soft term is M_3, the gluino mass. As $m_{1/2}$ increases, the gluino mass and squark masses increase, requiring more precise cancellations to reproduce the W mass, and thus greater electroweak fine-tuning.

Now that we have considered the different dark matter regions present within the CMSSM, we summarize the typical tunings in each case. We distinguish in table 3 the principal dark matter regions present within the CMSSM and the corresponding amounts of dark matter fine-tuning. With this as our starting point, we now consider the case of the NUHM model in which the universality between the soft Higgs masses and the soft sfermion masses is broken.

4. The NUHM

We now consider the MSSM with non-universal Higgs soft masses (NUHM) [12 – 14]. After breaking the universality between the soft Higgs and sfermion masses of the CMSSM we have the following independent inputs:

$$a_{\rm NUHM} = \left\{m_0,\ m_{H_1},\ m_{H_2},\ m_{1/2},\ A_0,\ \tan\beta,\ {\rm sign}(\mu)\right\}, \tag{4.1}$$

where m_{H_1} and m_{H_2} characterize the independent soft Higgs masses. These are subject to constraints arising from vacuum stability and cosmological considerations, and may be negative. As long as $m^2_{H_{1,2}} + \mu^2 > 0$ at the GUT scale, there is no dangerous high-scale vacuum state, but specifying the precise boundaries of the NUHM parameter space lies beyond the scope of this work.

As with the CMSSM, the NUHM contains a finite number of distinct regions in which it can provide the observed dark matter relic density, which were catalogued in [14]. Here we follow the approach of this previous work and reproduce the same regions of the parameter space. The plots we present here show the updated parameter space for the current world average for the top mass, $m_t = 170.9\,{\rm GeV}$, and include the current dark matter and δa_μ constraints. However, the primary goal of this work is rather to analyse the fine-tuning of the dark-matter regions of the NUHM. To this end we calculate and plot the dark-matter fine-tuning in the allowed parameter space, and also make some comments on the amount of electroweak fine-tuning.

As the NUHM contains the CMSSM as a limiting case, all the dark-matter regions present in the CMSSM are present in the NUHM. In addition, there are four new regions that are not present in the CMSSM:

- A pseudoscalar Higgs funnel at low $\tan\beta$.
- A bulk region where $\tilde\chi^0_1$ annihilation is dominantly mediated via t-channel $\tilde\tau$ exchange which does not violate Higgs mass bounds.
- A $\tilde\nu - \tilde\chi^0_1$ coannihilation region.
- A mixed bino/higgsino region at low m_0.

We shall be particularly interested in understanding how finely tuned the NUHM parameters must be in each of these new regions.

4.1 Comparison with the CMSSM

The NUHM contains all the points in the CMSSM parameter space. Therefore, we start by studying the tuning of the dark matter points A1-6, presented in tables 1, 2, with respect to the parameters of the NUHM.

We show the dark matter fine-tuning of these points with respect to the parameters $a_{\rm NUHM}$ in table 4. Point A1 represents the bulk region of the CMSSM, which is inaccessible because the Higgs is light. The primary annihilation channel is t-channel slepton exchange,

JHEP04(2008)099

Parameter	A1		A2		A3		A4	
	value	Δ^Ω	value	Δ^Ω	value	Δ^Ω	value	Δ^Ω
m_0	60	0.62	100	5.7	2030	200	540	8.1
m_{H_1}	60	0.017	100	0.26	2030	14	540	28
m_{H_2}	60	0.014	100	0.26	2030	230	540	30
$m_{1/2}$	200	0.99	500	5.8	500	18	600	8.0
$\tan\beta$	10	0.13	10	1.5	50	2.0	50	76
Δ_Ω		0.99		5.8		230		76
$\Delta_{\rm EW}$		37		190		1300		230

Parameter	A5		A6	
	value	Δ^Ω	value	Δ^Ω
m_0	277	23	1400	230
m_{H_1}	277	1.5	1400	10
m_{H_2}	277	2.5	1400	73
$m_{1/2}$	350	12	250	22
$\tan\beta$	50	48	50	8.2
Δ_Ω		48		230
$\Delta_{\rm EW}$		92		600

Table 4: A re-analysis of the representative points A1-6 from figures 1, 2, calculating their tunings with respect the NUHM rather than the CMSSM.

and the sensitivity in the CMSSM is primarily due to m_0 and $m_{1/2}$ as they determine the neutralino and slepton masses. This is also true in the NUHM, and the sensitivities to the Higgs soft masses are negligible.

Point A2 represents the low-$\tan\beta$ coannihilation region of the CMSSM, in which the primary sensitivities were to $m_{1/2}$ and m_0, as these determine the stau mass and the neutralino mass. Once again, this picture changes very little in the NUHM, with the sensitivity to the soft Higgs masses being negligible.

Points A3-6 have large $\tan\beta$. We recall that A3 and A6 lie in the higgsino-bino focus-point region. In the CMSSM the primary sensitivities were to m_0 and $m_{1/2}$, as m_0 (and to a lesser extent M_3) determine the size of μ, and $m_{1/2}$ determines $M_1(EW)$. Therefore these two parameters determine the mass and composition of the lightest neutralino, and the total CMSSM dark matter fine-tuning of the point in the CMSSM was $\Delta^\Omega = 27$. In the NUHM we have a very different picture. Here the total dark matter fine-tuning is $\Delta^\Omega = 230$, and the primary sensitivities are to m_0 and m_{H_2}. This can be explained by the process of radiative electroweak symmetry breaking. For electroweak symmetry breaking to occur, the Higgs (mass)^2 must become negative. By requiring this process to give the correct electroweak boson masses we set the size of μ, and thus the magnitude of the higgsino component of the lightest neutralino. Therefore to understand the sensitivity of a higgsino-bino dark matter region, we must look for the terms that contribute to the

JHEP04(2008)099

running of the Higgs mass-squared. First there is the soft Higgs mass at the GUT scale, and then there are the running effects, primarily the contribution from the stop mass. In the CMSSM, these two terms are coupled, reducing the dependence on either one individually. Therefore even though the scalar masses are large, the sensitivity of μ to m_0 remains small. In the NUHM there is no connection between the soft sfermion masses and the soft Higgs masses, therefore the sensitivity returns. Therefore one should not expect natural bino-higgsino dark matter at large m_0 in the NUHM. The significant increase in the electroweak fine-tuning for these points is due to exactly the same physics.

Points A4 and A5 represent the pseudoscalar Higgs funnel and the stau-coannihilation band. At this value of $\tan\beta$, the primary sensitivity is to $\tan\beta$, a feature not altered by breaking the universality amongst the scalars.

4.2 Detour: RGE behaviour with negative masses-squared

To understand the dependence of the dark matter phenomenology on the NUHM GUT scale parameters we need to understand how the soft Higgs masses affect the RGEs, and through them the low-energy parameters. Four low-energy parameters in particular are useful to consider when we talk about dark matter: μ, m_A, and $\tilde{\tau}_{L,R}$. The higgsino component of the LSP is determined by μ, m_A determines the position of the pseudoscalar Higgs funnel, and the lightest stau (a mixture of $\tilde{\tau}_{L,R}$) mediates the prevalent t-channel slepton exchange annihilation diagrams and determines the efficiency of $\tilde{\tau}$ coannihilation channels.

After EW symmetry breaking we can write μ as:

$$\mu^2 = \frac{m_{H_1}^2 - m_{H_2}^2 \tan^2\beta}{\tan^2\beta - 1} - \frac{1}{2}m_Z^2. \tag{4.2}$$

Clearly μ depends on the soft Higgs mass-squared terms and $\tan\beta$, as well as other soft parameters through the RGEs. It is also useful to consider the limit of large $\tan\beta$ where we can approximate (4.2) as:

$$\mu^2 = -m_{H_2}^2 + \frac{m_{H_1}^2}{\tan^2\beta}, \tag{4.3}$$

assuming $|m_{H_{1,2}}^2| \gg m_Z^2$. Therefore for large $\tan\beta$, to achieve REWSB and have $\mu^2 > 0$ we require either negative $m_{H_2}^2$, or very large positive $m_{H_1}^2$.

The pseudoscalar Higgs mass is determined after EWSB by the relation:

$$m_A^2 = m_{H_1}^2 + m_{H_2}^2 + 2\mu^2. \tag{4.4}$$

Clearly m_A^2 is strongly dependent upon the soft Higgs mass-squared terms, $\tan\beta$ through its effect on μ, and other soft terms through their influence on the Higgs RGEs.

We now consider the explicit form of the soft Higgs mass-squared RGEs:

$$\frac{d(m_{H_1}^2)}{dt} = \frac{1}{8\pi^2}\Big(- 3g_2^2M_2^2 - g_1^2M_1^2 + h_\tau^2(m_{\tilde{\tau}_L}^2 + m_{\tilde{\tau}_R}^2 + m_{H_1}^2 + A_\tau^2) \\ +3h_b^2(m_{\tilde{b}_L}^2 + m_{\tilde{b}_R}^2 + m_{H_1}^2 + A_b^2) - 2S\Big), \tag{4.5}$$

$$\frac{d(m_{H_2}^2)}{dt} = \frac{1}{8\pi^2}\left(-3g_2^2M_2^2 - g_1^2M_1^2 + 3h_t^2(m_{\tilde{t}_L}^2 + m_{\tilde{t}_R}^2 + m_{H_2}^2 + A_t^2) + 2S\right), \tag{4.6}$$

where S is definedly:

$$S \equiv \frac{g_1^2}{4}\left(m_{H_2}^2 - m_{H_1}^2 + 2\left(m_{\tilde{Q}_L}^2 - m_{\tilde{L}_L}^2 - 2m_{\tilde{u}_R}^2 + m_{\tilde{d}_R}^2 + m_{\tilde{e}_R}^2\right)\right.$$
$$\left. + \left(m_{\tilde{Q}_{3L}}^2 - m_{\tilde{L}_{3L}}^2 - 2m_{\tilde{t}_R}^2 + m_{\tilde{b}_R}^2 + m_{\tilde{\tau}_R}^2\right)\right). \quad (4.7)$$

The only parameters in these RGEs that we are not free to set at the GUT scale are the Yukawa couplings h_i. These are set by the requirement that the Higgs vevs should give the correct SM particle masses:

$$m_{\tau,b} = \frac{1}{\sqrt{2}} h_{\tau,b} v_1, \; m_t = \frac{1}{\sqrt{2}} h_t v_2. \quad (4.8)$$

Therefore $\tan\beta$ influences the RGEs indirectly through its determination of the size of the Yukawa couplings. The Yukawa couplings multiply the contribution to the RGEs from the soft squark and slepton mass-squared terms and the soft Higgs terms. Therefore varying the Yukawa couplings has a large impact on the running. As we increase $\tan\beta$, we increase v_2 with respect to v_1, and so we must decrease h_t and increase $h_{\tau,b}$. Therefore we reduce the Yukawa contribution to the running of $m_{H_2}^2$, while increasing the contribution to the running of $m_{H_1}^2$.

Now consider the RGEs for the right and left handed stau masses:

$$\frac{d(m_{\tilde{L}_{3L}}^2)}{dt} = \frac{1}{8\pi^2}\left(-3g_2^2 M_2^2 - g_1^2 M_1^2 + h_\tau^2\left(m_{\tilde{L}_{3L}}^2 + m_{\tilde{\tau}_R}^2 + m_{H_1}^2 + A_\tau^2\right) - 2S\right) \quad (4.9)$$

$$\frac{d(m_{\tilde{\tau}_R}^2)}{dt} = \frac{1}{8\pi^2}\left(-4g_1^2 M_1^2 + 2h_\tau^2\left(m_{\tilde{L}_{3L}}^2 + m_{\tilde{\tau}_R}^2 + m_{H_1}^2 + A_\tau^2\right) + 4S\right) \quad (4.10)$$

In both cases $m_{H_1}^2$ provides a substantial contribution to the running, with a coefficient of h_τ. As we have seen, increasing $\tan\beta$ increases h_τ and thus increases the impact of the Higgs masses on the running of the staus. Therefore we expect any effects of non-universal soft Higgs masses on the stau running to be amplified for large $\tan\beta$. In the CMSSM, $m_{H_1}^2$ will remain positive from the GUT scale to the EW scale. Indeed, it is harder to achieve REWSB if $m_{H_1}^2$ runs negative. Therefore generally this term provides a positive contribution to both the left and right handed stau RGE and acts to suppress the stau masses.

In the CMSSM this poses a problem. As we increase $\tan\beta$ we must increase the soft stau mass to avoid it becoming the LSP. However as we increase m_0 we are also increasing $m_{H_1}^2$, and thus increase the effect on the running. This can be avoided in the NUHM. We can set $m_{H_1}^2$ small and so avoid a very light $\tilde{\tau}$.

However, there is another more subtle effect. The interaction of the neutralinos with the stau also depends upon the composition of the lightest stau which is determined by the mixing between $\tilde{\tau}_{L,R}$. This mixing is increased if the two states are close in mass. In the CMSSM S is negligible and so $d(m_{\tilde{\tau}_R}^2)/dt \gg d(m_{\tilde{L}_{3L}}^2)/dt$, resulting in the right handed stau always being considerably lighter than the left-handed stau. In the NUHM we can avoid this by having a large negative S. This acts to suppress the left handed stau mass while increasing the right handed stau mass. As we increase the component of the left-handed stau, we increase the annihilation rate of neutralinos via t-channel stau exchange.

JHEP04(2008)099

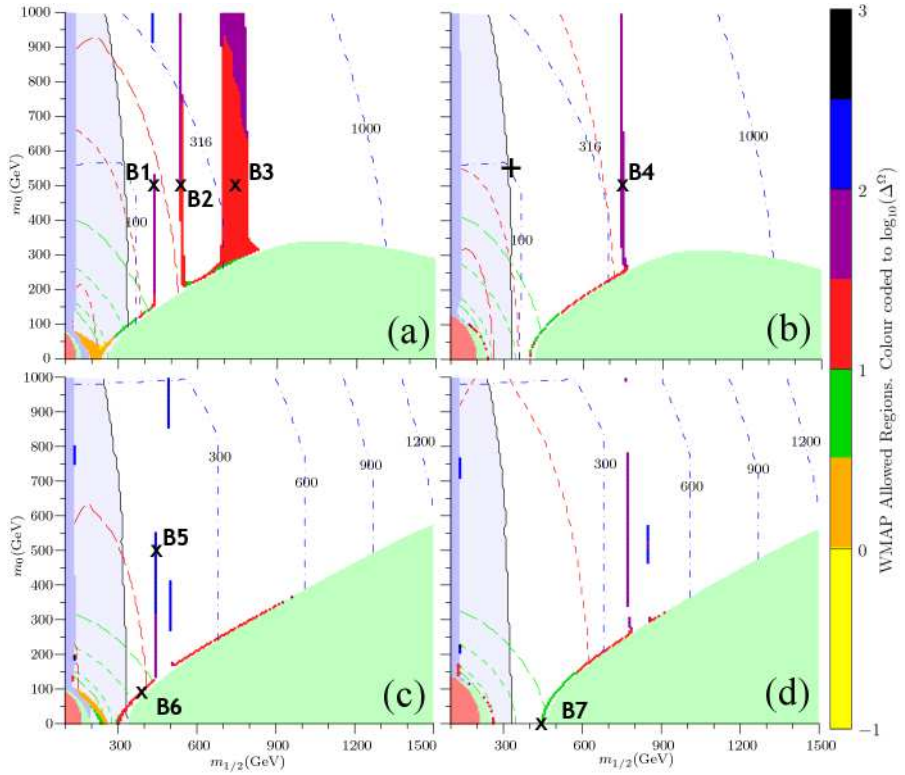

Figure 3: The $(m_0,\ m_{1/2})$ plane of the NUHM parameter space with $A_0 = 0$, $\tan\beta = 10$ and sign(μ) +ve. The values of μ and m_A vary between the panels: (a) $\mu = 400\,\text{GeV}$, $m_A = 400\,\text{GeV}$, (b) $\mu = 400\,\text{GeV}$, $m_A = 700\,\text{GeV}$, (c) $\mu = 700\,\text{GeV}$, $m_A = 400\,\text{GeV}$, (d) $\mu = 700\,\text{GeV}$, $m_A = 700\,\text{GeV}$. This figure can be compared directly to figure 2 in [14]. The Roman cross in panel (b) indicates the single point where the parameter space makes contact with the CMSSM.

4.3 Sample $(m_0, m_{1/2})$ planes in the NUHM

Having analysed the CMSSM points from the perspective of the NUHM, we now turn to a sampling of the full NUHM parameter space. In figure 3, we show $(m_{1/2}, m_0)$ planes for $\tan\beta = 10$, $A_0 = 0$ and sign(μ) positive. We set the electroweak scale parameters μ and m_A to different discrete values in each panel as explained in the figure caption.

As we saw in the previous section, μ and m_A are not high-scale inputs into the theory, rather they are the low-energy numbers derived from a given set of the true input parameters. However, displaying results as functions of these parameters can be more informative. As both have a strong dependence on $m^2_{H_{1,2}}$, we can fit a particular value of μ, m_A with the correct choice of $m^2_{H_{1,2}}$ at the GUT scale. Therefore we use a code that varies $m^2_{H_{1,2}}$ across the parameter space to fit the designated low-energy values of μ and m_A. All fine-tunings are calculated in terms of the inputs of the NUHM as listed in (4.1).

By starting with $(m_0, m_{1/2})$ planes, we make contact with the parameter space of the CMSSM as displayed in figures 1, 2.[5] As before, low m_0 is ruled out by a $\tilde{\tau}$ LSP

[5]We note in panel (b) of figure 3 the appearance of a CMSSM point, the only point in any of these

JHEP04(2008)099

Parameter	B1		B2		B3		B4	
	value	Δ^Ω	value	Δ^Ω	value	Δ^Ω	value	Δ^Ω
m_0	500	32	500	8.6	500	4.6	500	12
$m_{H_1}^2$	-80249	16	-126930	12	-248480	0.61	90625	2.3
$m_{H_2}^2$	461380	62	675760	25	1202900	24	1194100	60
$m_{1/2}$	435	39	540	19	750	18	750	38
$\tan\beta$	10	5	10	3.2	10	1.1	10	2.9
Δ_Ω		62		25		24		60
$\Delta_{\rm EW}$		150		220		390		390
μ	400	-	400	-	400	-	400	-
m_A	400	-	400	-	400	-	700	-

Parameter	B5		B6		B7	
	value	Δ^Ω	value	Δ^Ω	value	Δ^Ω
m_0	500	40	100	6.3	0	0
$m_{H_1}^2$	-416350	110	-400510	12	-79656	2.2
$m_{H_2}^2$	-24320	4.1	-332200	10	-266010	7.4
$m_{1/2}$	442	52	400	3.5	445	4.3
$\tan\beta$	10	5.8	10	0.55	10	1.9
Δ_Ω		110		12		7.4
$\Delta_{\rm EW}$		250		250		250
μ	700	-	700	-	700	-
m_A	400	-	400	-	700	-

Table 5: Analysis of the points B1-7, shown in figure 3, which are representative of the pseudoscalar Higgs funnel (B1,2,4,5), mixed bino-higgsino dark matter (B3) and $\tilde{\tau}$ coannihilation regions (B6,7). We present a breakdown of the dark matter fine-tuning with respect to each parameter of the NUHM. We give the value of $m_{H_{1,2}}^2$, but the tunings are calculated with respect to $m_{H_{1,2}}$.

(light green), and low $m_{1/2}$ results in a Higgs with $m_h < 111\,\text{GeV}$ (light grey with black boundary). As before, δa_μ favours light sleptons, and thus low m_0 and $m_{1/2}$.

The dark matter phenomenology shows some similarities to and some marked differences from the CMSSM. First, we see a familiar $\tilde{\tau}$ coannihilation region alongside the region with a $\tilde{\tau}$ LSP. As in the CMSSM, this region is plotted in red and green, designating a tuning of $\Delta^\Omega = 3 - 30$. The only new feature of the coannihilation region here is that effects of the non-universal Higgs soft masses alter the running of the stau mass, which allows access to regions with $m_0 = 0$. We can access $m_0 = 0$ with small negative $m_{H_1}^2$ and larger negative $m_{H_2}^2$. The combination of a small Yukawa contribution (due to low $\tan\beta$ along with small $|m_{H_1}^2|$) along with negative S results in the stau mass that increases as we run down from the GUT scale, allowing an acceptable stau mass even with $m_0 = 0$.

The points B6 and B7 are representative of the $\tilde{\tau}$ coannihilation region, and the break-

planes where full GUT-scale universality is recovered.

JHEP04(2008)099

downs of their tunings are also shown in table 5. The dependences on m_0 and $m_{1/2}$ are similar to what was observed in the CMSSM. However, the dominant sensitivities are now to $m_{H_{1,2}}$. For both these points the soft Higgs mass-squared terms are large and negative at the GUT scale. As we have seen, these soft parameters have a significant effect on the stau RGE. Therefore the coannihilation strip exhibits tuning with respect to these parameters. The total sensitivity remains low suggesting that, even though the soft Higgs masses play a role in the running, the dominant contribution to the stau mass is still from M_1.

More distinctive deviations from the familiar CMSSM phenomenology arise in the forms of the strong vertical dark matter regions at particular values of $m_{1/2}$. In panel (a) three vertical strips are present. To understand these lines we need to consider the mass and composition of the lightest neutralino. The bino component of the lightest neutralino is determined by $M_1(EW) \approx 0.4 m_{1/2}(GUT)$, whereas the wino component is determined by $M_2(EW) \approx 0.8 m_{1/2}(GUT)$. Hence, $M_2(EW) > M_1(EW)$ throughout the NUHM parameter space, and we never have a large wino component in the LSP. Of more importance is the higgsino component, determined by $\mu(EW)$. When $\mu(EW) \approx M_1(EW)$, there will be a sizeable higgsino component in the LSP. In panel (a) we have set $\mu = 400\,\mathrm{GeV}$ and $m_A = 400\,\mathrm{GeV}$. Therefore, when $m_{1/2} \approx 1000\,\mathrm{GeV}$, $M_1(EW) \approx \mu$ and the lightest neutralino will be a bino/higgsino mixture. However, for $m_{1/2} \gg 1000\,\mathrm{GeV}$ the lightest neutralino is mainly a higgsino, with a mass $m_{\tilde{\chi}_1^0} \approx 400\,\mathrm{GeV}$, whereas for $m_{1/2} \ll 1000\,\mathrm{GeV}$ the $\tilde{\chi}_1^0$ is predominantly a bino and has a mass determined by $M_1(EW)$.

With this in mind, we can understand the vertical lines in panel (a) at particular values of $m_{1/2}$. At $m_{1/2} = 500\,\mathrm{GeV}$, the lightest neutralino is a bino with a mass $m_{\tilde{\chi}_1^0} \approx 200\,\mathrm{GeV}$. As the pseudoscalar Higgs mass is $m_A = 400\,\mathrm{GeV}$ throughout, this results in resonant neutralino annihilation through the pseudoscalar Higgs. As a result, the relic density is below the WMAP value across the region $450 < m_{1/2} < 530$. On the edges of the resonance the relic density may fall within the narrow range favoured by astrophysics. The lines are mostly plotted in purple and blue, corresponding to a large degree of dark matter fine-tuning $\Delta^{\Omega} = 30 - 300$. However, it is interesting that the edge of the resonance at larger $m_{1/2}$ is plotted in red. This is the first instance of an acceptable pseudoscalar Higgs resonance region with relatively low dark-matter fine-tuning, thanks to the larger higgsino fraction in the LSP at larger $m_{1/2}$. Both the LSP mass and the mass of m_A are sensitive to μ, so the mass of the LSP and m_A are coupled. This mitigates the dark matter tuning of the pseudoscalar Higgs funnel to an extent.

Points B1 and B2 lie on either side of the pseudoscalar Higgs funnel, where it is interesting to break the dark matter fine-tuning measure down into its component parts. Unsurprisingly, the dark matter fine-tuning is due to a balancing act between the mass of the pseudoscalar Higgs, as shown by the large sensitivity to m_{H_2}, and the neutralino mass, as shown by the sensitivity to $m_{1/2}$.

The other vertical strip is a wide region around $m_{1/2} \approx 750\,\mathrm{GeV}$, where the predominantly bino LSP acquires a sufficient higgsino admixture to suppress the relic density to the observed value. This wide band is plotted in red and purple, representing a tuning of $10 - 30$, similar to that of the low-m_0 end of the bino/higgsino region within the CMSSM. There is also a thin line of green at the base of this band where it meets the coannihilation

JHEP04(2008)099

strip. This shows that the interaction of a stau coannihilation region with a bino/higgsino LSP reduces the overall tuning of either region alone.

Point B3 is representative of this region. The primary dark matter fine-tunings are clearly with respect to m_{H_2} and $m_{1/2}$. In this case, the dark matter fine-tuning is related to the balance between the roles of these terms in determining μ and M_1 at the electroweak scale. This is the first instance of a mixed bino-higgsino region at low m_0 that we find in the NUHM. It is therefore interesting to see that, even with a TeV-scale value of m_{H_2}, the tuning remains relatively small. This is in contrast to the point A3, at which a TeV-scale soft Higgs mass gave large fine-tuning. To understand the origin of both electroweak and dark matter fine-tunings, it is useful to consider the analytic form of the dependence of the low-energy parameter $\mu(EW)$ on the GUT-scale soft inputs. For $\tan\beta = 10$, we have:

$$\begin{aligned}\frac{m_Z^2}{2} = \; & -0.94\mu^2 + 0.010m_{H_1}^2 - 0.19M_2^2 - 0.0017M_1^2 - 0.63m_{H_2}^2 + 0.38m_{Q_3}^2 \\ & +0.38m_{U_3}^2 + 0.093A_t^2 - 0.011A_tM_1 - 0.070A_tM_2 - 0.30A_tM_3 \\ & +2.51M_3^2 + 0.0059M_1M_2 + 0.028M_1M_3 + 0.195M_2M_3, \end{aligned} \tag{4.11}$$

from which we can see that, when $m_{Q_3}^2 = m_{H_{1,2}}^2$, the terms from the scalars approximately cancel. This explains the jump in sensitivity when this universality is broken. On the other hand, in order to obtain a small value of μ, these soft scalar terms need to provide a large contribution to balance out the contribution from M_3^2. This explains why we find a higgsino/bino only at large m_0 in the CMSSM. In the NUHM, it is unnecessary to go to large m_0, just large $m_{H_2}^2$. By keeping m_0, and thus $m_{Q_3}^2$, small one keeps the dark matter and electroweak fine-tunings associated with these parameters under control. The remaining large electroweak fine-tuning associated with point B3 is due to $M_{1/2}$ being quite sizeable.

In panel (b) we have $\mu = 400\,\text{GeV}$ and $m_A = 700\,\text{GeV}$. Here we see only the lower edge of the pseudoscalar resonance. This band lies at 750 GeV and is plotted in purple, once again showing the large dark matter fine-tuning we expect of such resonances. The upper edge of the resonance never appears, because at larger $m_{1/2}$ the lightest neutralino is dominantly higgsino. Therefore, at values of $m_{1/2}$ above the resonance, the higgsino nature of the LSP suppresses the relic density so that the relic density never rises enough to fit the WMAP measurement.

Point B4 illustrates the component dark matter fine-tunings at the resonance. As with point B1, the dark matter fine-tuning is large, and primarily due to sensitivities to $m_{H_2}^2$ and $m_{1/2}$. These are due to their effects on the pseudoscalar Higgs mass and the mass of the LSP, respectively.

In panel (c) we set $\mu = 700\,\text{GeV}$ and $m_A = 400\,\text{GeV}$. As the pseudoscalar mass is the same, the pseudoscalar Higgs funnel is centred in the same place as in panel (a). However, the higgsino fraction of the LSP has dropped, increasing the overall relic density. Therefore one must go closer to the resonance before the enhancement to the annihilation cross section is sufficient to fit the observed relic density. Therefore the WMAP lines are closer to the peak of the resonance, and require more precise dark matter fine-tuning than for the lower value of μ. This is shown by examining the component dark matter fine-tunings for point

JHEP04(2008)099

B5. The dark matter fine-tuning is large, and primarily due to m_{H_2} through its influence on the pseudoscalar Higgs mass. In panel (c) there is no region in which the LSP is higgsino, due to the larger value of μ. One would have to go to $m_{1/2} \approx 1700\,\text{GeV}$ before the LSP acquires a significant higgsino fraction as $\mu = 700\,\text{GeV}$.

Finally, in panel (d) we take $\mu = 700\,\text{GeV}$ and $m_A = 700\,\text{GeV}$, and we see the pseudoscalar Higgs resonance at $m_{1/2} = 800\,\text{GeV}$ as expected, and it remains finely tuned, as before. As in panel (c), the value of μ is too large to find a region of the parameter space in which the neutralino is higgsino.

Overall, figure 3 shows some similarities and some marked deviations from the phenomenology of the CMSSM. A $\tilde{\tau}$ coannihilation band appears in roughly the same region of the parameter space and exhibits slightly larger tuning. This increase is due to the effect of the soft Higgs masses squared on the $\tilde{\tau}$ running. A further deviation from the CMSSM comes in the form of a pseudoscalar Higgs funnel at low $\tan\beta$. In most cases this exhibits dark matter fine-tuning similar to the CMSSM, supporting the observation that resonances require significant dark matter fine-tuning wherever they appear. The exception is when the LSP has a significant higgsino fraction. The sensitivity of both m_A and $m_{\tilde{\chi}_1^0}$ to μ lowers the required dark matter fine-tuning significantly. There also appears a band of higgsino/bino dark matter and we find that the tuning is of the same order as in the CMSSM, which is surprising. In the CMSSM the focus-point region has relatively low dark matter fine-tuning because of the cancellation among the scalar masses. By breaking this universality, this cancellation is broken. However, it also allows us to access mixed bino/higgsino regions at low m_0. This enhances other annihilation channels, such as that via t-channel slepton exchange, and we require a smaller higgsino admixture to obtain a suitable dark matter relic density. These regions recover the relatively low dark matter fine-tuning of the focus-point region of the CMSSM.

Finally, we note that we have also calculated the electroweak fine-tuning across these planes in the NUHM parameter space, and find it to be very similar to that of the CMSSM planes studied previously.

We now consider the behaviours of these regions as $\tan\beta$ increases. In figure 4 we take $\mu = 400\,\text{GeV}$, $m_A = 700\,\text{GeV}$, $A_0 = 0$ and $\text{sign}(\mu)$ positive, and in panels (a)-(d) we take successively larger values of $\tan\beta$.[6]

As the value of $\tan\beta$ increases, the mass and composition of the neutralino across the $(m_{1/2}, m_0)$ plane remains essentially unaltered. Therefore we find the lower edge of the pseudoscalar funnel in the same place in all panels. Studying the breakdown of the dark matter fine-tunings of the pseudoscalar Higgs funnel for large $\tan\beta$ at point B8, we find that in this case all parameters show a significant tuning. The primary tunings come from m_{H_2} and $\tan\beta$. From (4.4), (4.2) we can see that this comes from the dominant sensitivity of m_A^2, through μ, on both $\tan\beta$ and $m_{H_2}^2$.

The pseudoscalar Higgs funnel remains in the same place as $\tan\beta$ increases, whereas the $\tilde{\tau}$-coannihilation strip moves considerably. For larger $\tan\beta$ the Yukawa contribution to the stau running is enhanced. This suppresses the stau mass, requiring larger m_0 to avoid

[6]Note the CMSSM point in panel (a) of figure 4.

JHEP04(2008)099

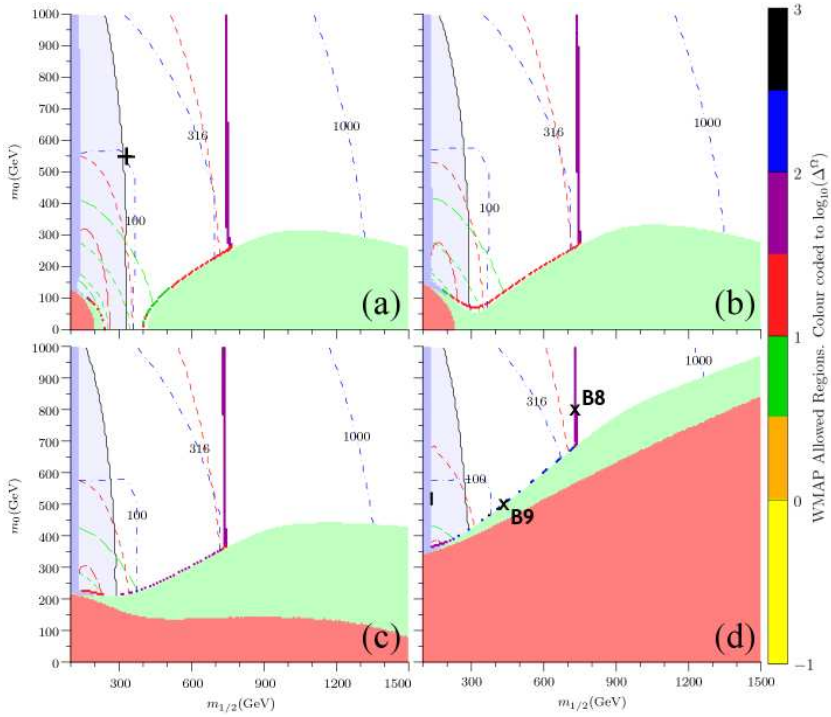

Figure 4: Sample $(m_{1/2}, m_0)$ planes of the NUHM parameter space with $A_0 = 0$, $\mu = 400\,\text{GeV}$, $m_A = 700\,\text{GeV}$ and sign(μ) and the following values of $\tan\beta$: (a) $\tan\beta = 10$, (b) $\tan\beta = 20$, (c) $\tan\beta = 35$, (d) $\tan\beta = 50$. The Roman cross in panel (a) shows the single point where the NUHM makes contact with the MSSM.

Parameter	B8		B9	
	value	Δ^Ω	value	Δ^Ω
m_0	800	21	500	150
$m_{H_1}^2$	1609600	30	892230	98
$m_{H_2}^2$	1357100	75	379620	1.3
$m_{1/2}$	730	14	432	35
$\tan\beta$	50	50	50	290
Δ_Ω		75		290
Δ_{EW}		420		130
μ	400	-	400	-
m_A	700	-	700	-

Table 6: Points B8 and B9, shown in figure 4 exemplify the behaviour of the pseudoscalar Higgs funnel (B8) and the stau-coannihilation region (B9) at large $\tan\beta$ within the NUHM. We present a breakdown of the dark matter fine-tuning with respect to each parameter of the NUHM. We give the value of $m_{H_{1,2}}^2$, although the tunings are calculated with respect to $m_{H_{1,2}}$.

a stau LSP. For very low m_0 there is a brick red region. This is not due to a failure of REWSB, but rather it is due to a tachyonic stau mass.

JHEP04(2008)099

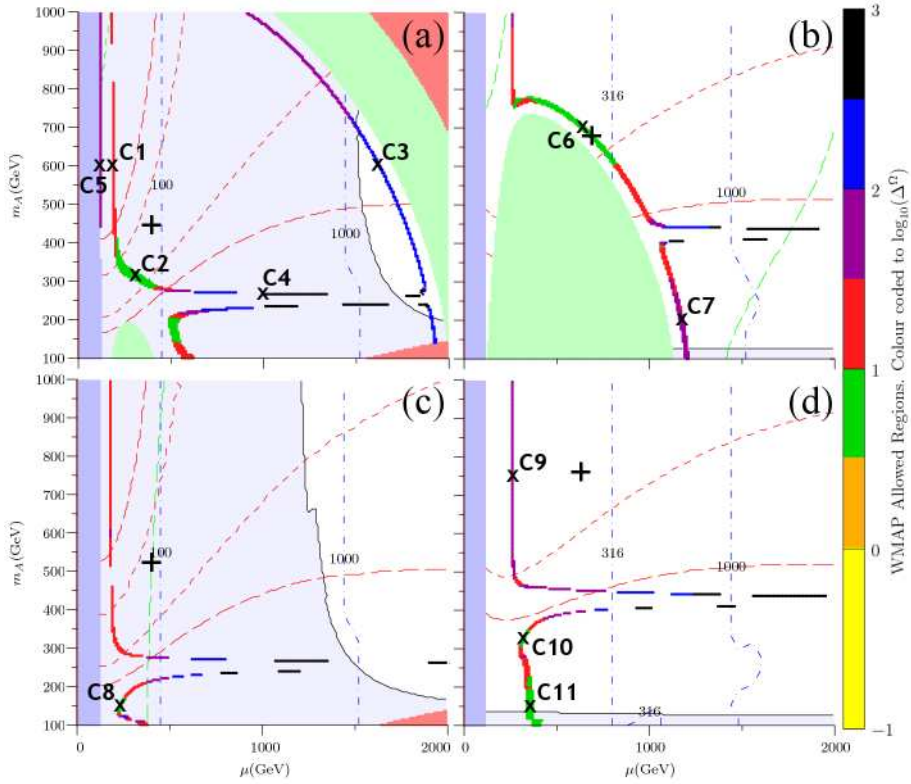

Figure 5: Sample NUHM (μ, m_A) planes with $A_0 = 0$, $\tan\beta = 10$ and sign(μ) positive, and different values of m_0 and $m_{1/2}$: (a) $m_0 = 100\,\text{GeV}$, $m_{1/2} = 300\,\text{GeV}$, (b) $m_0 = 100\,\text{GeV}$, $m_{1/2} = 500\,\text{GeV}$, (c) $m_0 = 300\,\text{GeV}$, $m_{1/2} = 300\,\text{GeV}$, (d) $m_0 = 300\,\text{GeV}$, $m_{1/2} = 500\,\text{GeV}$. The Roman crosses in each panel show where the NUHM meets the CMSSM.

By increasing $\tan\beta$ we reduce the dominance of M_1 in the running of the stau mass-squared. This breaks the link between the masses of the $\tilde{\tau}$ and the $\tilde{\chi}_1^0$, resulting in an increase of the tuning required for the coannihilation region at larger values of $\tan\beta$. Point B9 is representative of the $\tilde{\tau}$ coannihilation region at large $\tan\beta$. Though there is large sensitivity to the soft gaugino mass $m_{1/2}$, this is eclipsed by the sensitivities to $\tan\beta$ and m_0.

4.4 Sample (μ, m_A) planes

We now discuss other planes so as to explore more features of the NUHM model. In figure 5 we consider (μ, m_A) planes with $A_0 = 0$, $\tan\beta = 10$ and sign(μ) positive, taking different values of m_0 and $m_{1/2}$ in the various panels. As before, though we plot results in terms of μ and m_A, the primary variables are $m^2_{H_{1,2}}$.

We first consider some overall features. Low μ is ruled out in all cases by the appearance of a light chargino (light blue). In panels (a) and (c), the low value of $m_{1/2} = 300$ GeV results in a Higgs boson with $m_h < 111\,\text{GeV}$ across much of the parameter space. This bound is very sensitive to variations in the top mass, so regions that are excluded here

JHEP04(2008)099

could be allowed with a higher top mass. On the other hand, in panels (b) and (d), only very low values of m_A result in a problematically light Higgs. In panels (a) and (b), the low value of $m_0 = 100$ GeV results in a light $\tilde{\tau}$. This gives a region at low μ and m_A in which the $\tilde{\tau}$ is the LSP and as such is ruled out (light green). Finally, in panel (a) $m_{1/2}$ and m_0 are light enough to give light sneutrinos. For large μ and m_A, one of the sneutrinos becomes the LSP, ruling out this corner of the parameter space.[7]

Before considering the dark matter regions, we first note the composition of the lightest neutralino in different regions of the parameter space. In panels (a) and (c) $M_1(EW) \approx 120\,\text{GeV}$, whereas in panels (b) and (d) $M_1(EW) \approx 200\,\text{GeV}$. Therefore for $\mu \gg 120(200)\,\text{GeV}$ the LSP is predominantly a bino with a mass $m_{\tilde{\chi}_1^0} \approx 120(200)\,\text{GeV}$. Below these values of μ, the lightest neutralino acquires a significant higgsino fraction.

As before, the regions that fit the relic density favoured by WMAP are displayed with the corresponding dark matter fine-tuning colours. The vertical dark matter band at low μ in all panels features a mixed bino/higgsino dark matter particle, and is plotted in red and purple, corresponding to a dark matter fine-tuning $\Delta^\Omega \approx 20 - 40$. Points C1 and C9 are representative of the higgsino/bino band, and their dark matter fine-tunings are broken down in table 7. As one would expect, the fine-tuning is due to a balancing act between m_{H_2} and $m_{1/2}$, as these determine the composition of the lightest neutralino, and thus its annihilation rate.

Point C5 also represents a bino/higgsino region. It is unusual in that, normally, the larger the higgsino component, the more efficient the annihilation. However, in this case, as μ is lowered from point C1, the higgsino fraction increases and yet the dark matter relic density rises again. Indeed, C5 is almost evenly split between higgsino and bino components and yet it fits the WMAP relic density measurement. This is due to the fact that, as μ drops, the mass of the neutralino is lowered. At point C5 the LSP becomes lighter than the Z, shutting off the annihilation channel $\tilde{\chi}_1^0\tilde{\chi}_1^0 \to ZZ$. This reduces the annihilation cross section enough that the relic density is acceptable once more.

Another region that is easy to pick out is the pseudoscalar Higgs funnel along $m_A = 240(400)\,\text{GeV}$ for $m_{1/2} = 300(500)\,\text{GeV}$ respectively. As before, these funnels require significant dark matter fine-tuning and as such are predominantly plotted in blue and black, showing a tuning $\Delta^\Omega > 100$. Point C4 is a representative point whose dark matter fine-tuning breakdown we display in table 7. In previous pseudoscalar Higgs regions the dark matter fine-tuning was due primarily to $m_{H_{1,2}}$ and $m_{1/2}$. Here we find that the sensitivity to the Higgs masses has increased significantly. From (4.4) this is easy to understand. If we increase μ while keeping m_A the same we must carefully balance the large $m_{H_{1,2}}^2$ contributions to give the required m_A. This careful balancing manifests as a steadily increasing sensitivity of m_A to the Higgs soft masses as we increase μ. This translates to a large sensitivity of the pseudoscalar Higgs funnel.

At the other end of the spectrum, there is a region of the pseudoscalar Higgs funnel at

[7] Sneutrinos are massive, neutral and weakly-interacting, and so could in principle account for the dark matter. However, they generally give $\Omega_{\text{CDM}}h^2 \ll \Omega_{\text{CDM}}^{\text{WMAP}}h^2$. This can be avoided in some models with right-handed neutrinos, but this possibility lies beyond the scope of the MSSM, so we do not consider it further here.

JHEP04(2008)099

Parameter	C1		C2		C3		C4	
	value	Δ^Ω	value	Δ^Ω	value	Δ^Ω	value	Δ^Ω
m_0	100	0.99	100	4.7	100	13	100	2.7
$m_{H_1}^2$	279530	0.38	-27130	0.99	-2289300	79	-966510	390
$m_{H_2}^2$	188070	17	111220	3.5	-3637400	110	-1248800	330
$m_{1/2}$	300	16	300	0.20	300	30	300	46
$\tan\beta$	10	0.8	10	0.51	10	0.57	10	1.4
Δ_Ω		17		4.7		110		390
$\Delta_{\rm EW}$		74		73		1300		500
μ	190	-	300	-	1620	-	1000	-
m_A	600	-	315	-	600	-	268	-

Parameter	C5		C6		C7		C8	
	value	Δ^Ω	value	Δ^Ω	value	Δ^Ω	value	Δ^Ω
m_0	100	3.3	100	5.6	100	4.7	300	0.64
$m_{H_1}^2$	319380	2.7	-22696	0.59	-1445500	35	-70487	6.7
$m_{H_2}^2$	222330	76	-25802	0.68	-1440300	34	246160	2.4
$m_{1/2}$	300	85	500	5.6	500	3.4	300	3.6
$\tan\beta$	10	2.7	10	1.3	10	0.068	10	1.2
Δ_Ω		85		5.6		35		6.7
$\Delta_{\rm EW}$		74		210		590		79
μ	120	-	640	-	1170	-	235	-
m_A	600	-	700	-	200	-	150	-

Parameter	C9		C10		C11	
	value	Δ^Ω	value	Δ^Ω	value	Δ^Ω
m_0	300	6.1	300	0.55	300	1.3
$m_{H_1}^2$	401250	0.62	-106330	5.1	-211970	0.067
$m_{H_2}^2$	568170	40	525900	2.5	497010	6.8
$m_{1/2}$	500	31	500	0.023	500	6.5
$\tan\beta$	10	1.5	10	1.0	10	0.30
Δ_Ω		40		5.1		6.8
$\Delta_{\rm EW}$		180		180		180
μ	260	-	320	-	350	-
m_A	750	-	325	-	150	-

Table 7: Points C1-11, shown in figure 5, illustrate the behaviour of mixed bino-higgsino dark matter (C1,5,9), sneutrino coannihilation (C3), the pseudoscalar Higgs funnel (C4), stau-coannihilation (C2,6,7,11), and the pseudoscalar funnel region with a mixed bino-higgsino LSP (C8,10). We present breakdowns of the dark matter fine-tuning with respect to each parameter of the NUHM. We give the value of $m_{H_{1,2}}^2$, but the fine-tunings are calculated with respect to $m_{H_{1,2}}$.

JHEP04(2008)099

low μ with remarkably low tuning. This occurs when there is a significant higgsino fraction in the LSP, such as at points C8 and C10. In this region, both m_A and the neutralino mass are sensitive to μ. This results in the mass of the neutralino and the pseudoscalar being coupled, and reduces the sensitivity of the mass difference $\Delta_m = m_A - 2m_{\tilde{\chi}_1^0}$. At points C8 and C10 the dominant annihilation channels are to heavy quarks via an s-channel pseudoscalar Higgs. Remarkably the total dark matter fine-tunings of the points are only 6.7 and 5.1 respectively.

As the $\tilde{\nu}_{e,\mu}$ become the LSPs in the large μ, large m_A region of panel (a), there is a corresponding sneutrino coannihilation region lying parallel to its boundary, which is plotted in purple and blue indicating a dark matter fine-tuning $\Delta^\Omega > 80$. Point C3 is a representative of this region, whose dark matter fine-tuning breakdown is also displayed in table 7. The dark matter fine-tuning is large, and comes primarily from the Higgs sector. It is the existence of large negative $m_{H_1}^2$ that allows for light sneutrinos. Thus the sneutrino masses are very sensitive to the Higgs soft mass-squared parameters, and this is reflected in the dark matter fine-tuning. There is also some dark matter fine-tuning with respect to $m_{1/2}$ that is typical of the need to balance the bino mass against that of a coannihilation partner with an uncorrelated mass.

Finally, the light $\tilde{\tau}$ at low μ and m_0 has an effect on the dark matter relic density. As the mass of the $\tilde{\tau}$ is reduced, the annihilation cross section is increased via t-channel slepton exchange. Also, as one approaches the region in which the stau is the LSP, there are additional contributions from $\tilde{\tau} - \tilde{\chi}_1^0$ coannihilation processes. These two effects combine to give dark matter bands along the edges of the stau LSP region in panels (a) and (b). Points C2 in panel (a) and C6,7 in panel (b) are representative points. At point C2 the annihilation proceeds through equal parts of t-channel $\tilde{e}_R$, $\tilde{\mu}_R$, $\tilde{\tau}$ annihilation (15-20% each), annihilation to $b, \overline{b}$ via off-shell pseudoscalar Higgs bosons (18%) and $\tilde{\tau}$ coannihilation (15%). Only the coannihilation processes would be expected to exhibit a high sensitivity to the soft parameters, as t-channel processes are fairly insensitive and the point is far from the pseudoscalar resonance, reducing significantly the sensitivity of the s-channel pseudoscalar process. As a result, we have a region that arises from a mixture of channels and exhibits low tuning. The subdominant role of coannihilation explains why there is so little dark matter fine-tuning with respect to $m_{1/2}$. The role of the stau in both the coannihilation and t-channel processes explains the dominant dark matter fine-tuning with respect to m_0, and the dependence on m_{H_2} appears from running effects.

Unfortunately, point C2 results in a light Higgs with $m_h = 110\,\text{GeV}$, which is probably unacceptably low, even allowing for the theoretical uncertainty in the calculation of its mass. On the other hand, panel (b) has a larger value of $m_{1/2}$ and hence Higgs mass. However, the masses of the LSP and the sleptons are also increased. This decreases the slepton t-channel annihilation cross sections, requiring larger contributions from processes that are finely tuned in order to fit the WMAP relic density, which is apparent at points C6 and C7.[8] At point C6, t-channel slepton annihilation only accounts for 3% of the annihilation rate via each channel (9% overall). The remaining 91% is made up entirely of

[8]We note that there is a CMSSM point very close to C6

JHEP04(2008)099

coannihilation processes, dominantly with $\tilde{\tau}$, but also $\tilde{e}_R, \tilde{\mu}_R$. As this plane has low m_0, the slepton masses are predominantly determined by $m_{1/2}$. Once again, there is the familiar pattern of dark matter fine-tunings for a low-$\tan\beta$, low-m_0 slepton coannihilation region. The overall dark matter fine-tuning is low, and what fine-tuning does exists is due to m_0 and $m_{1/2}$. Point C7 tells a slightly different story. The pattern of annihilation channels is almost identical to C6, and we see the typical dark matter fine-tunings of a coannihilation region in the sensitivity to m_0 and $m_{1/2}$. However, the dark matter fine-tuning with respect to $m_{H_{1,2}}$ has increased dramatically, due to the massive increase in $m^2_{H_{1,2}}$ between points C6 and C7. Now the stau running is dominated by the Higgs mass-squared terms rather than the gaugino mass, and the coannihilation region becomes fine-tuned once again.

There is one further interesting region. In panel (d) at low m_A there is a kink in the higgsino/bino region. The band moves to larger μ and the dark matter fine-tuning drops dramatically. The band is plotted in green rather than purple, indicating a dark matter fine-tuning of less than 10. The kink in the band appears at $m_A = 280$ GeV. Around this region the LSP is predominantly a bino with a small but significant higgsino component, and the LSP has a mass of around 200 GeV. As the pseudoscalar mass drops, the masses of the heavy Higgs, H, and the charged Higgses, $H^{\pm}$, also decrease. Around $m_A = 280\,\text{GeV}$, the annihilation channels $\tilde{\chi}^0_1\tilde{\chi}^0_1 \to hA, W^{\pm}H^{\mp}, ZH$ open up, which are kinematically forbidden at larger m_A. These can progress through either t-channel neutralino (chargino) exchange or s-channel Higgs and Z processes. They require a small higgsino component, but significantly less than the higgsino/bino region represented by point C9. This balance of the higgsino and bino components of the LSP appears in the sensitivity of point C11 on $m_{1/2}$ and m_{H_2}. Thus C11 represents a higgsino/bino region with low dark matter fine-tuning - something that does not exist in the CMSSM. This is because a large negative $m^2_{H_1}$ is needed to achieve low $m_{A,H,H^{\pm}}$.

We now consider in figure 6 the behaviours of these regions as $\tan\beta$ increases. We have set $m_0 = 100\,\text{GeV}$, $m_{1/2} = 300\,\text{GeV}$, $A_0 = 0$ and increase $\tan\beta$ in steps in each panel.

We note first the bulk features of the plane. As noted previously, increasing $\tan\beta$ decreases the mass of the lightest stau. Thus plots at larger $\tan\beta$ have larger regions ruled out because the LSP is a $\tilde{\tau}$, and we do not show very large $\tan\beta$ because at $\tan\beta = 50$ the stau mass becomes tachyonic across the entire plane. By $\tan\beta = 35$ the light stau rules out all the parameter space below $\mu = 200\,\text{GeV}$. The mass of the light Higgs is also sensitive to $\tan\beta$, and is in all cases very close to $m_h = 111\,\text{GeV}$, so it only takes a small shift to cause a significant change in the area plotted in light grey.

The most significant change in the dark matter phenomenology is due to the varying $\tilde{\tau}$ mass. Between panels (a) and (b) the stau bulk/coannihilation region moves to larger μ and m_A. We also find a significant stau region at large m_A. These features are represented by points C15 and C14 respectively.[9] Comparing C15 directly to C2, we see from table 8 that the dark matter fine-tuning is due primarily to m_0 and $\tan\beta$. This is because these parameters determine the mass of the lighter stau and this is the primary source of sensitivity for bulk regions. There is also a degree of sensitivity to $m_{1/2}$, as there is a significant

[9]We note that there is a CMSSM point very close to C15.

JHEP04(2008)099

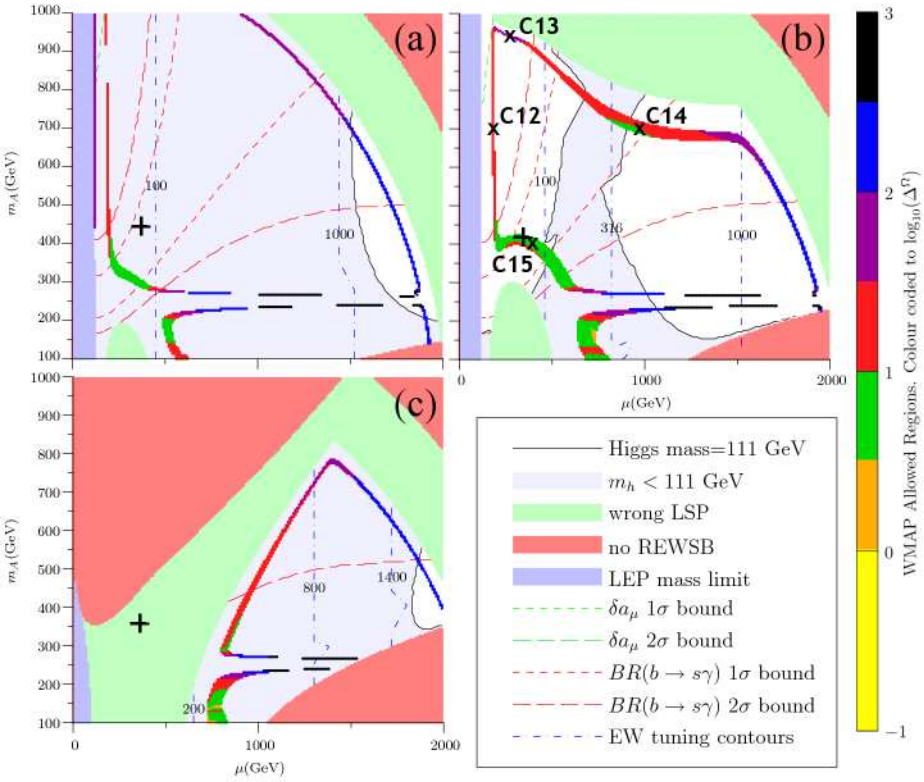

Figure 6: Sample NUHM (μ, m_A) planes with $A_0 = 0$, $m_0 = 100\,\text{GeV}$, $m_{1/2} = 300\,\text{GeV}$ and sign(μ) positive, and the following values of $\tan\beta$: (a) $\tan\beta = 10$, (b) $\tan\beta = 20$, (c) $\tan\beta = 35$. We do not show a plot for $\tan\beta = 50$ as the parameter space is entirely excluded. The Roman crosses in each panel show where the NUHM meets the CMSSM.

coannihilation contribution that requires the LSP and stau mass to be balanced. At point C14 one has similar degrees of dark matter fine-tuning with respect to $\tan\beta$, $m_{1/2}$ and m_0. However, there is now also large dark matter fine-tuning with respect to $m_{H_{1,2}}$, due to the larger magnitude of the soft higgsino mass-squared terms. The stau mass in this region becomes highly sensitive to $m^2_{H_2}$.

The other regions are little changed from before. Point C12 exemplifies the mixed bino/higgsino region at increasing $\tan\beta$. It can be compared directly to point C1, and we see that the component dark matter fine-tunings are virtually identical. Point C13 is representative of the sneutrino coannihilation region and can be compared to point C3. Once again the dark matter fine-tuning is due primarily to the soft Higgs masses through their impacts on the running of the sneutrino masses.

Much of the low-m_0 parameter space is forbidden by a light Higgs and/or a light stau. We now consider the effect of increasing $\tan\beta$ in a more open part of the parameter space. We take figure 5(d) with $m_0 = 300\,\text{GeV}$, $m_{1/2} = 500\,\text{GeV}$ as a starting point and increase $\tan\beta$ steadily, as seen in figure 7. In contrast to figure 6, the bulk features remain fairly stable for moderate values of $\tan\beta$. The first hint of a change appears in panel (c) at

JHEP04(2008)099

Parameter	C12		C13		C14		C15	
	value	Δ^Ω	value	Δ^Ω	value	Δ^Ω	value	Δ^Ω
m_0	100	1.0	100	15	100	7.2	100	8.7
$m_{H_1}^2$	477840	1.4	858150	48	-532000	6.5	-14857	0.28
$m_{H_2}^2$	175680	17	96420	6.3	-1263800	12	-2379	0.041
$m_{1/2}$	300	16	300	32	300	10	300	4.6
$\tan\beta$	20	0.56	20	21	20	8.7	20	6.5
Δ_Ω		17		48		12		8.7
$\Delta_{\rm EW}$		71		71		480		78
μ	185	-	275	-	1000	-	400	-
m_A	700	-	940	-	700	-	400	-

Table 8: Points C12-15, shown in figure 6, are representative of the higgsino/bino region (C12), the sneutrino coannihilation region (C13) and the stau-coannihilation/bulk region (C15,14) with increasing $\tan\beta$ within the NUHM. We present a breakdown of the dark matter fine-tuning with respect to each parameter of the NUHM. We give the value of $m_{H_{1,2}}^2$ but the tunings are calculated with respect to $m_{H_{1,2}}$.

Parameter	C16		C17		C18		C19	
	value	Δ^Ω	value	Δ^Ω	value	Δ^Ω	value	Δ^Ω
m_0	300	1.0	300	0.94	300	52	300	37
$m_{H_1}^2$	-47935	2.0	-170090	0.86	1021100	22	-52957	4.4
$m_{H_2}^2$	518240	3.8	475340	4.2	390800	0.58	-281880	2.3
$m_{1/2}$	500	3.1	500	3.7	500	25	500	20
$\tan\beta$	20	3.0	20	0.21	35	86	50	49
Δ_Ω		3.8		4.2		86		49
$\Delta_{\rm EW}$		170		170		170		290
μ	315	-	360	-	380	-	780	-
m_A	325	-	150	-	950	-	600	-

Table 9: Points C16-19, shown in figure 7, illustrate the behaviours of the mixed bino-higgsino, the pseudoscalar Higgs funnel (C16) and the stau-coannihilation/bulk regions (C17,18,19) at increasing values of $\tan\beta$ within the NUHM. We present a breakdown of the dark matter fine-tuning with respect to each parameter of the NUHM. We give the value of $m_{H_{1,2}}^2$, but the tunings are calculated with respect to $m_{H_{1,2}}$.

$\tan\beta = 35$, where we see a small region at large m_A in which the stau is the LSP. This expands to cut off low μ for $\tan\beta = 50$.

There are few dark matter surprises at larger $\tan\beta$. The pseudoscalar Higgs funnel and mixed higgsino/bino regions remain relatively unaltered throughout. The interaction of the pseudoscalar Higgs funnel with the higgsino/bino LSP continues to provide a favourable degree of tuning in panels (b) and (c). We take point C16 as a representative point, and break the tuning down in table 9. As for point C10, the tuning is small and the annihilation

JHEP04(2008)099

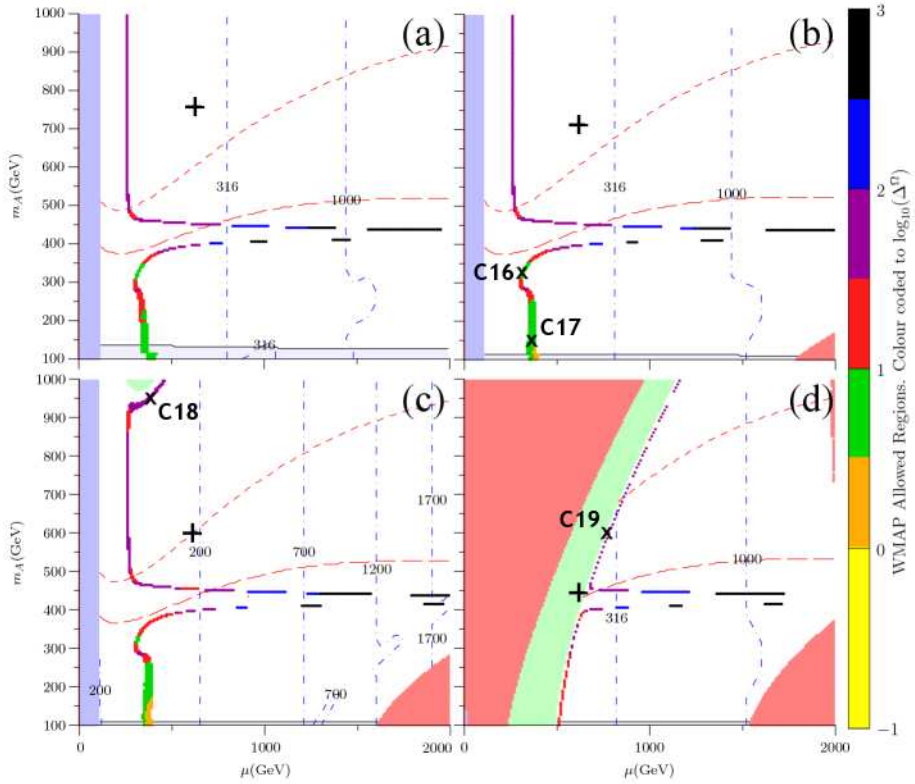

Figure 7: Sample NUHM (μ, m_A) planes with $A_0 = 0$, $m_0 = 300\,\text{GeV}$, $m_{1/2} = 500\,\text{GeV}$, sign($\mu$) positive and different values of $\tan\beta$: (a) $\tan\beta = 10$, (b) $\tan\beta = 20$, (c) $\tan\beta = 35$, (d) $\tan\beta = 50$. The Roman crosses in each panel show where the NUHM meets the CMSSM.

is primarily due to annihilation to heavy quarks via an s-channel pseudoscalar Higgs.

Point C17 exemplifies the behaviour of a predominantly bino LSP with a small higgsino admixture that can annihilate to hA, ZH and $W^{\pm}H\mp$. As with point C11, the dark matter fine-tuning is small and mostly due to the composition of the LSP, through $m_{1/2}$ and m_{H_2}.

Point C18 is in the new stau coannihilation region that appears at large $\tan\beta$. For $m_0 = 300\,\text{GeV}$, $m_{1/2} = 500\,\text{GeV}$ the staus are too heavy to contribute significantly to t-channel slepton exchange, so this region is pure coannihilation. The stau mass is mainly determined by m_0 and $\tan\beta$, and must be balanced against a predominantly bino LSP. Therefore, the tuning is dominated by $\tan\beta$ and m_0 with a secondary dependence on $m_{1/2}$. The coannihilation grows significantly by $\tan\beta = 50$ and point C19 represents this trend. As with point C18, we find the tuning to be due to m_0 and $\tan\beta$, with a secondary dependence on $m_{1/2}$.

Throughout all of these parameter scans we have also calculated the electroweak fine-tuning and found it to be of the same order as that found in the CMSSM for typical scales of soft masses considered.

JHEP04(2008)099

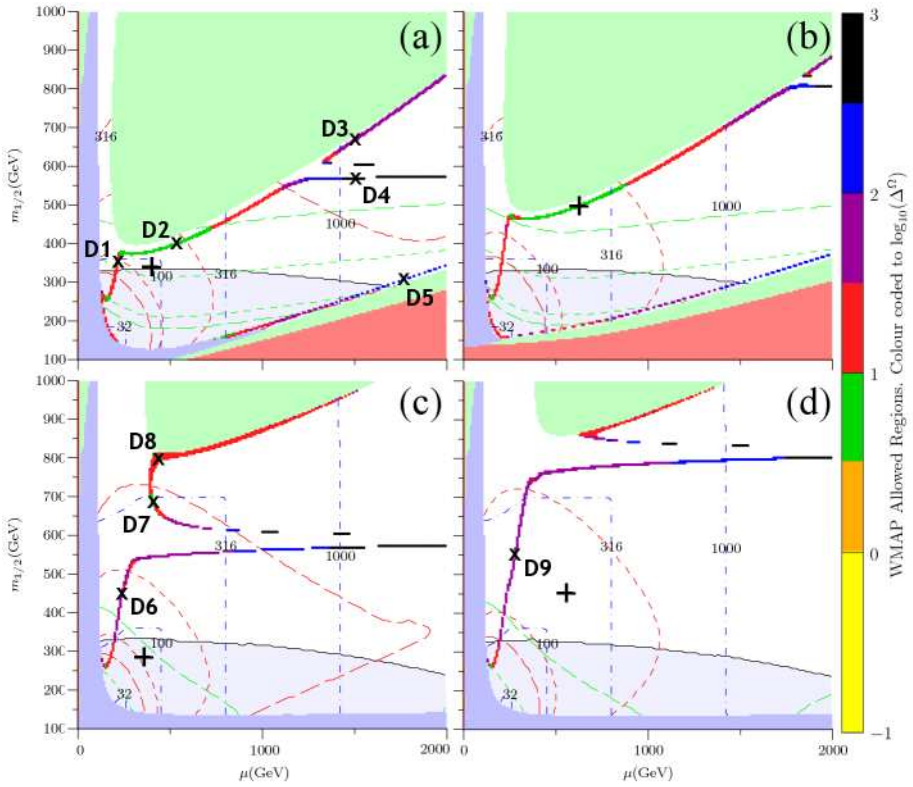

Figure 8: Sample NUHM (μ, $m_{1/2}$) planes with $A_0 = 0$, $\tan\beta = 10$, sign(μ) positive and varying m_0 and m_A: (a) $m_0 = 100\,\text{GeV}$, $m_A = 500\,\text{GeV}$, (b) $m_0 = 100\,\text{GeV}$, $m_A = 700\,\text{GeV}$, (c) $m_0 = 300\,\text{GeV}$, $m_A = 500\,\text{GeV}$, (d) $m_0 = 300\,\text{GeV}$, $m_A = 700\,\text{GeV}$. The Roman crosses in each panel show where the NUHM meets the CMSSM.

4.5 Sample $(\mu, m_{1/2})$ planes

Finally,we consider sample (μ, $m_{1/2}$) planes in the NUHM. These are interesting, e.g., because μ and $m_{1/2}$ are the parameters that determine the mass and composition of the lightest neutralino.[10]

In figure 8 we set $A_0 = 0$, $\tan\beta = 10$ and take discrete values of m_0 and m_A. We see that either low μ or low $m_{1/2}$ results in a light chargino that violates particle searches (light blue). Low $m_{1/2}$ also results in problems with a light Higgs (light grey with a black boundary). On the other hand, large $m_{1/2}$ results in a neutralino with a mass above that of the stau (light green). The exception is low μ where the neutralino is a higgsino and $m_{\tilde{\chi}_1^0}$ is insensitive to $m_{1/2}$. In panels (a) and (b) we have $m_0 = 100\,\text{GeV}$. This, combined with low $m_{1/2}$ and large μ results in a region in which the LSP is a sneutrino (light green).

We see once again the familiar dark matter regions of the previous plots. The pseudoscalar Higgs funnel appears as a pair of horizontal lines and exhibits large dark matter fine-tuning, and is characterized by the point D4 in table 10. Here we see that the large

[10]Note that in the following plots $m_{1/2}$ is the GUT-scale soft mass, whereas μ is the electroweak-scale Higgs term. This is in contrast to the plots of [14] where the plots were in terms of $M_2(EW)$ and $\mu(EW)$.

JHEP04(2008)099

Parameter	D1		D2		D3		D4	
	value	Δ^Ω	value	Δ^Ω	value	Δ^Ω	value	Δ^Ω
m_0	100	1.0	100	7.2	100	3.6	100	1.1
$m_{H_1}^2$	160370	0.30	-97736	3.3	-2206600	39	-2147800	360
$m_{H_2}^2$	255000	18	-20502	0.70	-2345100	41	-2588200	300
$m_{1/2}$	350	17	400	4.7	670	5.9	570	59
$\tan\beta$	10	0.51	10	1.1	10	0.027	10	0.070
Δ_Ω		18		7.2		41		360
$\Delta_{\rm EW}$		96		140		1100		1100
μ	210	-	530	-	1500	-	1500	-
m_A	500	-	500	-	500	-	500	-

Parameter	D5		D6		D7		D8	
	value	Δ^Ω	value	Δ^Ω	value	Δ^Ω	value	Δ^Ω
m_0	100	13	300	7.1	300	0.38	300	7.4
$m_{H_1}^2$	-2963700	110	109920	0.42	-120550	5.7	-216760	0.91
$m_{H_2}^2$	-4438200	140	490790	39	845460	5.1	1153100	9.0
$m_{1/2}$	310	32	450	30	680	4.7	800	2.6
$\tan\beta$	10	0.52	10	1.1	10	1.9	10	0.70
Δ_Ω		140		39		5.7		9.0
$\Delta_{\rm EW}$		1600		160		300		400
μ	1785	-	240	-	410	-	430	-
m_A	500	-	500	-	500	-	500	-

Parameter	D9	
	value	Δ^Ω
m_0	300	5.6
$m_{H_1}^2$	291010	0.38
$m_{H_2}^2$	661620	42
$m_{1/2}$	550	34
$\tan\beta$	10	1.4
Δ_Ω		42
$\Delta_{\rm EW}$		210
μ	280	-
m_A	700	-

Table 10: Points D1-9, shown in figure 8, are representative of bino-higgsino dark matter (D1,6,9), stau-coannihilation (D2,3,8), the pseudoscalar Higgs funnel (D4) and its interaction with mixed bino-higgsino dark matter (D7), and sneutrino coannihilation (D5). We present breakdowns of the dark matter fine-tuning with respect to each parameter of the NUHM. We give the value of $m_{H_{1,2}}^2$ but the tunings are calculated with respect to $m_{H_{1,2}}$.

JHEP04(2008)099

dark matter fine-tuning is due to the soft Higgs masses through their influence on m_A, and to $m_{1/2}$ through its influence on the neutralino mass.

The exception to this large dark matter fine-tuning is where the pseudoscalar funnel interacts with a higgsino/bino LSP and there is a small corner with low fine-tuning, as characterized by point D7. The annihilation here is mainly to heavy quarks via an s-channel pseudoscalar Higgs, and yet the total tuning is only 5.7. As noted previously, this relatively small dark matter fine-tuning comes from the common sensitivity of m_A and $m_{\tilde{\chi}_1^0}$ on μ.

There is also a $\tilde{\tau}$ coannihilation region in all four plots, which lies alongside the region ruled out due to a stau LSP. It exhibits similar tuning to the CMSSM. We break down the dark matter fine-tunings of this region at points D2 and D3, finding that at both points the tuning with respect to m_0 and $m_{1/2}$ is standard for a stau coannihilation strip at low m_0.[11] Point D3 has larger tuning because this region of parameter space requires large negative soft Higgs masses, which now dominate the determination of the mass of the light stau.

The sneutrino coannihilation region shows up alongside the sneutrino LSP region. Once again we find it to require significant dark matter fine-tuning, although this decreases steadily as one moves to lower μ. Point D5 is a representative point with, as before, large dark matter fine-tuning that depends on the soft Higgs masses.

Each plot also has a dark matter region at low μ that lies along a diagonal in the $(\mu, m_{1/2})$ plane, incorporating points D1,6,9. These regions are mixed bino/higgsino regions. In all cases the pseudoscalar Higgs and heavy Higgs bosons are sufficiently massive that annihilation of the mixed LSP proceeds mainly through the channels $\tilde{\chi}_1^0\tilde{\chi}_1^0 \to W^+W^-(ZZ)$, via t-channel chargino (neutralino) exchange. This process is very sensitive to the composition of the LSP and the masses of the exchanged particles. Therefore there is significant dark matter fine-tuning with respect to m_{H_2} and $m_{1/2}$ at all these points.

Finally, we consider the point D8 where the coannihilation strip and the mixed bino/higgsino strips meet. The combination of annihilation channels has a beneficial effect, with the overall dark matter fine-tuning dropping to 9.

Once again it is interesting to go beyond $\tan\beta = 10$, to understand how the phenomenology changes with $\tan\beta$. In figure 9 we consider $(\mu, m_{1/2})$ planes with $m_0 = 100\,\text{GeV}$, $m_A = 500\,\text{GeV}$ and steadily increasing values of $\tan\beta$. As we saw before, increasing $\tan\beta$ decreases the $\tilde{\tau}$ mass, causing the stau LSP regions to encroach on the parameter space. By $\tan\beta = 35$ the light stau rules out all values of low μ. As noted earlier, at such a low value of m_0, $\tan\beta = 50$ has a tachyonic stau and so is not shown here.

The change in the stau mass is the dominant factor that changes the dark matter phenomenology. With the lighter stau, the contribution to neutralino annihilation from t-channel stau exchange increases. We consider two points D10 and D11 in panel (b). At point D10 the annihilation is still dominated by coannihilation effects, but the growing contribution from t-channel stau exchange helps to lower the dark matter tuning. The

[11] This is also true for the CMSSM point seen in panel (b).

JHEP04(2008)099

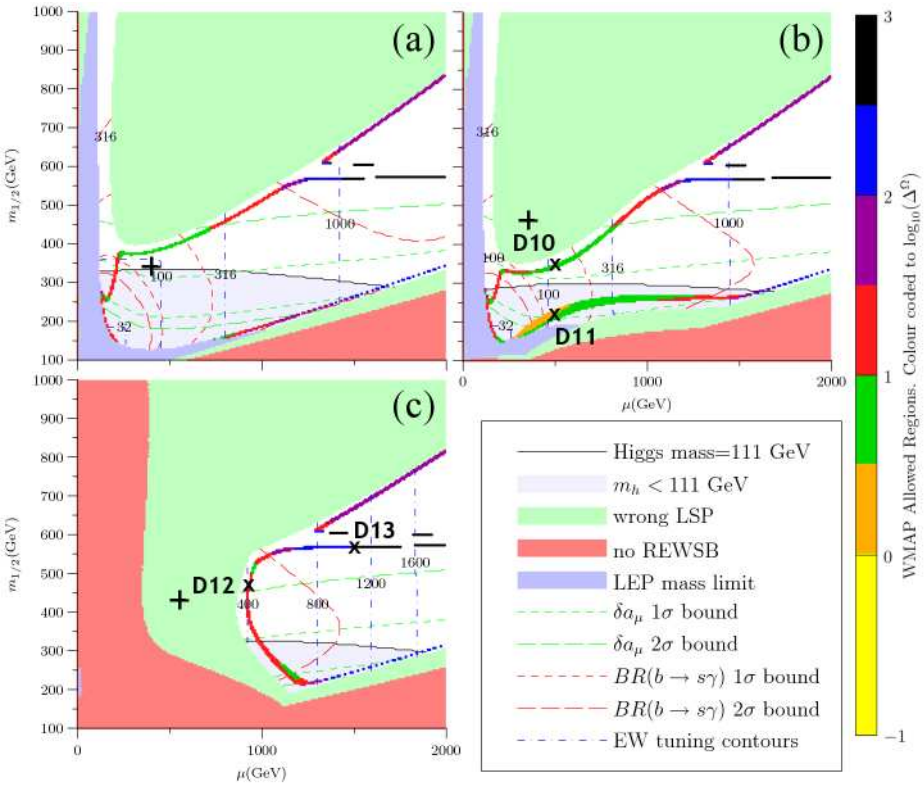

Figure 9: Sample NUHM (μ, $m_{1/2}$) planes with $A_0 = 0$, $m_0 = 100\,\text{GeV}$, $m_A = 500\,\text{GeV}$, sign(μ) positive and $\tan\beta$ varying: (a) $\tan\beta = 10$, (b) $\tan\beta = 20$, (c) $\tan\beta = 35$. We do not show a plane for $\tan\beta = 50$, as this part of the parameter space is entirely excluded. The Roman crosses in each panel show where the NUHM meets the CMSSM.

dark matter fine-tuning is predominantly due to m_0 and $\tan\beta$ through their influence on the mass of the lighter stau, with a subsidiary fine-tuning with respect to $m_{1/2}$. In contrast, point D11 lies in a dark matter band where the annihilation of neutralinos is dominantly through t-channel slepton exchange. As a result the dark matter fine-tuning is small, and due primarily to m_0 and $\tan\beta$ through their influence on the slepton masses.

As we move to larger $\tan\beta$, the coannihilation and bulk regions meet. In panel (c) we take point D12 as a representative of the meeting of these two regions. However, by this stage one needs large soft Higgs mass-squared parameters and the stau mass is sensitive to these, rather than to m_0 and $m_{1/2}$. Therefore there is large fine-tuning with respect to m_{H_1}. Finally, point D13 is representative point of the pseudoscalar Higgs funnel for large $\tan\beta$. As before, we find the dark matter fine-tuning to be large and predominantly due to the soft Higgs masses. This chimes with the general behaviour of the pseudoscalar Higgs funnel throughout our study.

5. Conclusions

We summarize in table 12 the ranges of dark matter fine-tunings found in the different dark

JHEP04(2008)099

Parameter	D10		D11		D12		D13	
	value	Δ^Ω	value	Δ^Ω	value	Δ^Ω	value	Δ^Ω
m_0	100	8.8	100	2.6	100	5.0	100	0.69
$m_{H_1}^2$	-21261	0.37	-377	0.0	-658190	15	-2200200	320
$m_{H_2}^2$	-73998	1.5	-243830	0.91	-772520	0.27	-2597000	280
$m_{1/2}$	345	4.7	220	2.1	470	4.1	567	32
$\tan\beta$	20	8.5	20	3.1	35	0.99	35	11
Δ_Ω		8.8		3.1		15		320
$\Delta_{\rm EW}$		120		120		420		1100
μ	500	-	500	-	930	-	1500	-
m_A	500	-	500	-	500	-	500	-

Table 11: Properties of points D10-13, shown in figure 9 which are representative of the pseudoscalar Higgs funnel (D13) and the stau-coannihilation/bulk region (D10,11,12) at increasing $\tan\beta$ within the NUHM. We present a breakdown of the dark matter fine-tuning with respect to each parameter of the NUHM. We give the value of $m_{H_{1,2}}^2$ but the tunings are calculated with respect to $m_{H_{1,2}}$.

Region	**Typical Δ^Ω**
$\tilde{\tau}$ bulk region	1-5
$\tilde{\tau} - \tilde{\chi}_1^0$ coannihilation	4-80
Bino annihilation via pseudoscalar Higgs Funnel	30-1200+
Bino/higgsino annihilation via pseudoscalar Higgs Funnel	3-10
Bino/higgsino region, $m_{\tilde{\chi}_1^0} > m_{H,A}$	30-300
Bino/higgsino region, $m_{\tilde{\chi}_1^0} < m_{H,A}$	2-10
$\tilde{\nu} - \tilde{\chi}_1^0$ coannihilation	15-200

Table 12: A summary of the different dark matter regions present within the NUHM and typical values of the corresponding dark matter fine-tunings. We also note that combinations from many channels decrease the overall tuning.

matter regions appearing in the NUHM, which may be compared to those found previously in the CMSSM, as shown in tables 1, 2 and summarised in table 3. Comparing first the bulk regions, which require the smallest amounts of dark matter fine-tuning in both the CMSSM and the NUHM, we see that CMSSM point A2 has a low amount of dark matter fine-tuning that is at the end of the range found in the NUHM. However, point A2 has too small a value of m_h, and hence is not acceptable, whereas the NUHM can circumvent this restriction. Thus, *the NUHM provides access to dark matter which is less fine-tuned than in the CMSSM.* Turning then to the $\tilde{\tau}$ coannihilation regions, we see that the NUHM offers an option of lower fine-tuning than that found in the CMSSM at point A5. For reasons explained earlier in the text, there are very large variations in the amounts of dark matter fine-tuning required in the pseudoscalar Higgs funnel region of the NUHM, and the amount found at the CMSSM point A4 lies within this range. In addition, the NUHM

JHEP04(2008)099

contains a region in which a bino/higgsino LSP annihilates via a pseudoscalar Higgs boson that requires dramatically less fine-tuning than the pseudoscalar funnel in the CMSSM. Likewise, NUHM analogues of the focus points A3 and A6 shown in table 2 require dark matter fine-tunings that are substantially less than in the CMSSM. One new region appears in the NUHM that has no CMSSM analogue, namely the $\tilde{\nu} - \tilde{\chi}_1^0$ coannihilation region. At least in the examples studied, this requires rather more dark matter fine-tuning than the $\tilde{\tau} - \tilde{\chi}_1^0$ coannihilation region.

Although it was not the primary focus of this paper, we have also calculated the electroweak fine-tuning across the NUHM parameter space, and found it to be of the same order of magnitude as in other MSSM studies.

Generally speaking, the fact that the NUHM has more parameters offers more possibilities to find regions with particularly small (or large) dark matter fine-tunings. The smaller amounts of dark matter fine-tuning generally occur in regions where several different (co)annihilation processes contribute to the final dark matter density, e.g., where a bino/higgsino band meets a stau coannihilation region. Conversely, there are instances where a tight correlation is necessary between two *a priori* independent MSSM parameters, such as the stau and neutralino masses along a coannihilation strip, which is imposed automatically in the lower-dimensional parameter space of the CMSSM, resulting in smaller amount of dark matter fine-tuning than might otherwise have been expected.

There have been several studies of the implications of prospective LHC and/or ILC measurements for the accuracy with which the astrophysical dark matter density could be calculated on the basis of collider measurements [11]. These studies have emphasized relatively favourable points in the CMSSM coannihilation region at low $m_{1/2}$, where the dark matter fine-tuning is relatively low and the prospective collider measurements relatively accurate. Our analysis offers some prognosis as to which NUHM regions might be favourable for extensions of these analyses. Clearly, the presence of NUHM points with low dark matter fine-tuning and relatively light sparticles is encouraging *a priori*. However, we note that in general the NUHM relic density is sensitive to the separate and independent values of the soft Higgs masses $m_{H_{1,2}}$. Detailed consideration of their determinations using collider data has not yet been given, as far as we know, and we recall that the prospects for measuring directly the masses of the heavier Higgs bosons at the LHC and ILC are limited, though the prospects of the latter would be improved with the $\gamma - \gamma$ option, or by going to higher energies as at CLIC.

The extension of these collider dark matter studies to the NUHM is a large task that lies beyond the scope of this paper. However, this exploratory study has revealed some of the prospective opportunities and pitfalls.

Acknowledgments

JPR would like to thank Ben Allanach for useful advice. The work of JPR was funded under the FP6 Marie Curie contract MTKD-CT-2005-029466. We also acknowledge partial support from the following grants: PPARC Rolling Grant PPA/G/S/2003/00096; EU Network MRTN-CT-2004-503369; EU ILIAS RII3-CT-2004-506222

JHEP04(2008)099

References

[1] J.R. Ellis, K. Enqvist, D.V. Nanopoulos and F. Zwirner, *Observables in low-energy superstring models*, *Mod. Phys. Lett.* **A 1** (1986) 57;
R. Barbieri and G.F. Giudice, *Upper bounds on supersymmetric particle masses*, *Nucl. Phys.* **B 306** (1988) 63.

[2] D.J.H. Chung et al., *The soft supersymmetry-breaking lagrangian: theory and applications*, *Phys. Rept.* **407** (2005) 1 [hep-ph/0312378].

[3] J.R. Ellis, J.S. Hagelin, D.V. Nanopoulos, K.A. Olive and M. Srednicki, *Supersymmetric relics from the Big Bang*, *Nucl. Phys.* **B 238** (1984) 453;
see also H. Goldberg, *Constraint on the photino mass from cosmology*, *Phys. Rev. Lett.* **50** (1983) 1419.

[4] G. Jungman, M. Kamionkowski and K. Griest, *Supersymmetric dark matter*, *Phys. Rept.* **267** (1996) 195 [hep-ph/9506380].

[5] J.R. Ellis, K. Enqvist, D.V. Nanopoulos and K. Tamvakis, *Gaugino masses and grand unification*, *Phys. Lett.* **B 155** (1985) 381;
M. Drees, *Phenomenological consequences of $N = 1$ supergravity theories with nonminimal kinetic energy terms for vector superfields*, *Phys. Lett.* **B 158** (1985) 409.

[6] G.W. Anderson and D.J. Castano, *Challenging weak scale supersymmetry at colliders*, *Phys. Rev.* **D 53** (1996) 2403 [hep-ph/9509212]; *Naturalness and superpartner masses or when to give up on weak scale supersymmetry*, *Phys. Rev.* **D 52** (1995) 1693 [hep-ph/9412322]; *Measures of fine tuning*, *Phys. Lett.* **B 347** (1995) 300 [hep-ph/9409419];
G.G. Ross and R.G. Roberts, *Minimal supersymmetric unification predictions*, *Nucl. Phys.* **B 377** (1992) 571;
B. de Carlos and J.A. Casas, *One loop analysis of the electroweak breaking in supersymmetric models and the fine tuning problem*, *Phys. Lett.* **B 309** (1993) 320 [hep-ph/9303291];
S. Dimopoulos and G.F. Giudice, *Naturalness constraints in supersymmetric theories with nonuniversal soft terms*, *Phys. Lett.* **B 357** (1995) 573 [hep-ph/9507282];
P.H. Chankowski, J.R. Ellis and S. Pokorski, *The fine-tuning price of LEP*, *Phys. Lett.* **B 423** (1998) 327 [hep-ph/9712234];
R. Barbieri and A. Strumia, *About the fine-tuning price of LEP*, *Phys. Lett.* **B 433** (1998) 63 [hep-ph/9801353];
P.H. Chankowski, J.R. Ellis, M. Olechowski and S. Pokorski, *Haggling over the fine-tuning price of LEP*, *Nucl. Phys.* **B 544** (1999) 39 [hep-ph/9808275];
G.L. Kane and S.F. King, *Naturalness implications of LEP results*, *Phys. Lett.* **B 451** (1999) 113 [hep-ph/9810374];
J.L. Feng, K.T. Matchev and T. Moroi, *Multi-TeV scalars are natural in minimal supergravity*, *Phys. Rev. Lett.* **84** (2000) 2322 [hep-ph/9908309]; *Focus points and naturalness in supersymmetry*, *Phys. Rev.* **D 61** (2000) 075005 [hep-ph/9909334];
M. Bastero-Gil, G.L. Kane and S.F. King, *Fine-tuning constraints on supergravity models*, *Phys. Lett.* **B 474** (2000) 103 [hep-ph/9910506];
A. Romanino and A. Strumia, *Are heavy scalars natural in minimal supergravity?*, *Phys. Lett.* **B 487** (2000) 165 [hep-ph/9912301];
J.A. Casas, J.R. Espinosa and I. Hidalgo, *The MSSM fine tuning problem: a way out*, *JHEP* **01** (2004) 008 [hep-ph/0310137];
B.C. Allanach and C.G. Lester, *Multi-dimensional mSUGRA likelihood maps*, *Phys. Rev.* **D 73** (2006) 015013 [hep-ph/0507283];

JHEP04(2008)099

B.C. Allanach, *Naturalness priors and fits to the constrained minimal supersymmetric standard model*, *Phys. Lett.* **B 635** (2006) 123 [hep-ph/0601089];
P. Athron and D.J. Miller, *A new measure of fine tuning*, *Phys. Rev.* **D 76** (2007) 075010 [arXiv:0705.2241].

[7] J.R. Ellis and K.A. Olive, *How finely tuned is supersymmetric dark matter?*, *Phys. Lett.* **B 514** (2001) 114 [hep-ph/0105004]; *Constraining supersymmetry*, *New J. Phys.* **4** (2002) 32 [hep-ph/0202110];
J.R. Ellis, S. Heinemeyer, K.A. Olive and G. Weiglein, *Indirect sensitivities to the scale of supersymmetry*, *JHEP* **02** (2005) 013 [hep-ph/0411216].

[8] S.F. King and J.P. Roberts, *Natural implementation of neutralino dark matter*, *JHEP* **09** (2006) 036 [hep-ph/0603095]; *Natural dark matter*, *Acta Phys. Polon.* **B38** (2007) 607 [hep-ph/0609147].

[9] S.F. King and J.P. Roberts, *Natural dark matter from type-I string theory*, *JHEP* **01** (2007) 024 [hep-ph/0608135].

[10] S.F. King, J.P. Roberts and D.P. Roy, *Natural dark matter in SUSY GUTs with non-universal gaugino masses*, *JHEP* **10** (2007) 106 [arXiv:0705.4219].

[11] M. Battaglia et al., *Updated post-WMAP benchmarks for supersymmetry*, *Eur. Phys. J.* **C 33** (2004) 273 [hep-ph/0306219];
E.A. Baltz, M. Battaglia, M.E. Peskin and T. Wizansky, *Determination of dark matter properties at high-energy colliders*, *Phys. Rev.* **D 74** (2006) 103521 [hep-ph/0602187].

[12] V. Berezinsky et al., *Neutralino dark matter in supersymmetric models with nonuniversal scalar mass terms*, *Astropart. Phys.* **5** (1996) 1 [hep-ph/9508249];
P. Nath and R. Arnowitt, *Non-universal soft SUSY breaking and dark matter*, *Phys. Rev.* **D 56** (1997) 2820 [hep-ph/9701301];
M. Drees, M.M. Nojiri, D.P. Roy and Y. Yamada, *Light Higgsino dark matter*, *Phys. Rev.* **D 56** (1997) 276 [*Erratum ibid.* **64** (1997) 039901] [hep-ph/9701219];
see also M. Drees et al., *Scrutinizing LSP dark matter at the LHC*, *Phys. Rev.* **D 63** (2001) 035008 [hep-ph/0007202];
J.R. Ellis, T. Falk, G. Ganis, K.A. Olive and M. Schmitt, *Charginos and neutralinos in the light of radiative corrections: sealing the fate of Higgsino dark matter*, *Phys. Rev.* **D 58** (1998) 095002 [hep-ph/9801445];
J.R. Ellis, T. Falk, G. Ganis and K.A. Olive, *Supersymmetric dark matter in the light of LEP and the Tevatron collider*, *Phys. Rev.* **D 62** (2000) 075010 [hep-ph/0004169];
R. Arnowitt, B. Dutta and Y. Santoso, *Coannihilation effects in supergravity and D-brane models*, *Nucl. Phys.* **B 606** (2001) 59 [hep-ph/0102181];
V.D. Barger, M.S. Berger and P. Ohmann, *The Supersymmetric particle spectrum*, *Phys. Rev.* **D 49** (1994) 4908 [hep-ph/9311269];
W. de Boer, R. Ehret and D.I. Kazakov, *Predictions of SUSY masses in the minimal supersymmetric grand unified theory*, *Z. Physik* **C 67** (1995) 647 [hep-ph/9405342];
V. Bertin, E. Nezri and J. Orloff, *Neutralino dark matter beyond CMSSM universality*, *JHEP* **02** (2003) 046 [hep-ph/0210034];
H. Baer, A. Mustafayev, S. Profumo, A. Belyaev and X. Tata, *Neutralino cold dark matter in a one parameter extension of the minimal supergravity model*, *Phys. Rev.* **D 71** (2005) 095008 [hep-ph/0412059];

JHEP04(2008)099

H. Baer, A. Mustafayev, S. Profumo, A. Belyaev and X. Tata, *Direct, indirect and collider detection of neutralino dark matter in SUSY models with non-universal Higgs masses*, *JHEP* **07** (2005) 065 [hep-ph/0504001].

[13] J.R. Ellis, K.A. Olive and Y. Santoso, *The MSSM parameter space with non-universal Higgs masses*, *Phys. Lett.* **B 539** (2002) 107 [hep-ph/0204192].

[14] J.R. Ellis, T. Falk, K.A. Olive and Y. Santoso, *Exploration of the MSSM with non-universal Higgs masses*, *Nucl. Phys.* **B 652** (2003) 259 [hep-ph/0210205].

[15] G.L. Kane, C.F. Kolda, L. Roszkowski and J.D. Wells, *Study of constrained minimal supersymmetry*, *Phys. Rev.* **D 49** (1994) 6173 [hep-ph/9312272].

[16] J.R. Ellis, T. Falk, K.A. Olive and M. Srednicki, *Calculations of neutralino stau coannihilation channels and the cosmologically relevant region of MSSM parameter space*, *Astropart. Phys.* **13** (2000) 181 [*Erratum ibid.* **15** (2001) 413] [hep-ph/9905481];
J.R. Ellis, T. Falk and K.A. Olive, *Neutralino stau coannihilation and the cosmological upper limit on the mass of the lightest supersymmetric particle*, *Phys. Lett.* **B 444** (1998) 367 [hep-ph/9810360];
M.E. Gómez, G. Lazarides and C. Pallis, *Supersymmetric cold dark matter with Yukawa unification*, *Phys. Rev.* **D 61** (2000) 123512 [hep-ph/9907261];
M.E. Gómez, G. Lazarides and C. Pallis, *Yukawa unification,* $b \to s\gamma$ *and bino stau coannihilation*, *Phys. Lett.* **B 487** (2000) 313 [hep-ph/0004028]; *Yukawa quasi-unification*, *Nucl. Phys.* **B 638** (2002) 165 [hep-ph/0203131];
T. Nihei, L. Roszkowski and R. Ruiz de Austri, *Exact cross sections for the neutralino slepton coannihilation*, *JHEP* **07** (2002) 024 [hep-ph/0206266];
S. Mizuta and M. Yamaguchi, *Coannihilation effects and relic abundance of Higgsino dominant* LSP_s, *Phys. Lett.* **B 298** (1993) 120 [hep-ph/9208251];
J. Edsjo and P. Gondolo, *Neutralino relic density including coannihilations*, *Phys. Rev.* **D 56** (1997) 1879 [hep-ph/9704361];
A. Birkedal-Hansen and E.-H. Jeong, *Gaugino and Higgsino coannihilations. I: neutralino neutralino interactions*, *JHEP* **02** (2003) 047 [hep-ph/0210041];
H. Baer, C. Balázs and A. Belyaev, *Neutralino relic density in minimal supergravity with co-annihilations*, *JHEP* **03** (2002) 042 [hep-ph/0202076];
G. Bélanger, F. Boudjema, A. Pukhov and A. Semenov, *MicrOMEGAs: a program for calculating the relic density in the MSSM*, *Comput. Phys. Commun.* **149** (2002) 103 [hep-ph/0112278];
J.R. Ellis, T. Falk, G. Ganis, K.A. Olive and M. Srednicki, *The CMSSM parameter space at large* $\tan\beta$, *Phys. Lett.* **B 510** (2001) 236 [hep-ph/0102098];
J.R. Ellis, K.A. Olive and Y. Santoso, *Constraining supersymmetry*, *New J. Phys.* **4** (20002) 32 [hep-ph/0202110];
M. Drees and M.M. Nojiri, *The Neutralino relic density in minimal* $N = 1$ *supergravity*, *Phys. Rev.* **D 47** (1993) 376 [hep-ph/9207234];
H. Baer and M. Brhlik, *Cosmological relic density from minimal supergravity with implications for collider physics*, *Phys. Rev.* **D 53** (1996) 597 [hep-ph/9508321]; *Neutralino dark matter in minimal supergravity: direct detection vs. collider searches*, *Phys. Rev.* **D 57** (1998) 567 [hep-ph/9706509];
H. Baer et al., *Yukawa unified supersymmetric* SO(10) *model: cosmology, rare decays and collider searches*, *Phys. Rev.* **D 63** (2001) 015007 [hep-ph/0005027];
A.B. Lahanas, D.V. Nanopoulos and V.C. Spanos, *Neutralino dark matter elastic scattering in a flat and accelerating universe*, *Mod. Phys. Lett.* **A 16** (2001) 1229 [hep-ph/0009065];

JHEP04(2008)099

J.R. Ellis, D.V. Nanopoulos and K.A. Olive, *Lower limits on soft supersymmetry-breaking scalar masses*, *Phys. Lett.* **B 525** (2002) 308 [hep-ph/0109288];
J.R. Ellis, T. Falk, K.A. Olive and M. Schmitt, *Supersymmetric dark matter in the light of LEP 1.5*, *Phys. Lett.* **B 388** (1996) 97 [hep-ph/9607292];
J.L. Feng, K.T. Matchev and T. Moroi, *Multi-TeV scalars are natural in minimal supergravity*, *Phys. Rev. Lett.* **84** (2000) 2322 [hep-ph/9908309];
J.L. Feng, K.T. Matchev and T. Moroi, *Focus points and naturalness in supersymmetry*, *Phys. Rev.* **D 61** (2000) 075005 [hep-ph/9909334];
J.L. Feng, K.T. Matchev and F. Wilczek, *Neutralino dark matter in focus point supersymmetry*, *Phys. Lett.* **B 482** (2000) 388 [hep-ph/0004043];
K. Griest and D. Seckel, *Three exceptions in the calculation of relic abundances*, *Phys. Rev.* **D 43** (1991) 3191;
J.R. Ellis, T. Falk, K.A. Olive and M. Srednicki, *Calculations of neutralino stau coannihilation channels and the cosmologically relevant region of MSSM parameter space*, *Astropart. Phys.* **13** (2000) 181 [*Erratum ibid.* **15** (2001) 413] [hep-ph/9905481].

[17] S.P. Martin and M.T. Vaughn, *Two loop renormalization group equations for soft supersymmetry breaking couplings*, *Phys. Rev.* **D 50** (1994) 2282 [hep-ph/9311340].

[18] B.C. Allanach, *SOFTSUSY: a C++ program for calculating supersymmetric spectra*, *Comput. Phys. Commun.* **143** (2002) 305 [hep-ph/0104145].

[19] G. Bélanger, F. Boudjema, A. Pukhov and A. Semenov, *MicrOMEGAs: a program for calculating the relic density in the MSSM*, *Comput. Phys. Commun.* **149** (2002) 103 [hep-ph/0112278]; *MicrOMEGAs*2.0*: a program to calculate the relic density of dark matter in a generic model*, *Comput. Phys. Commun.* **176** (2007) 367 [hep-ph/0607059].

[20] B.C. Allanach, A. Djouadi, J.L. Kneur, W. Porod and P. Slavich, *Precise determination of the neutral Higgs boson masses in the MSSM*, *JHEP* **09** (2004) 044 [hep-ph/0406166].

[21] J.P. Miller, E. de Rafael and B.L. Roberts, *Muon $g-2$: review of theory and experiment*, *Rept. Prog. Phys.* **70** (2007) 795 [hep-ph/0703049];
Muon g-2 collaboration, G.W. Bennett et al., *Measurement of the negative muon anomalous magnetic moment to* 0.7 *ppm*, *Phys. Rev. Lett.* **92** (2004) 161802 [hep-ex/0401008]; *Measurement of the positive muon anomalous magnetic moment to* 0.7 *ppm*, *Phys. Rev. Lett.* **89** (2002) 101804 [*Erratum ibid.* **89** (2002) 129903] [hep-ex/0208001];
M. Davier, S. Eidelman, A. Hocker and Z. Zhang, *Confronting spectral functions from e^+e^- annihilation and τ decays: consequences for the muon magnetic moment*, *Eur. Phys. J.* **C 27** (2003) 497 [hep-ph/0208177];
see also K. Hagiwara, A.D. Martin, D. Nomura and T. Teubner, *The SM prediction of $g-2$ of the muon*, *Phys. Lett.* **B 557** (2003) 69 [hep-ph/0209187];
F. Jegerlehner, unpublished, as reported in M. Krawczyk, *Precision muon $g-2$ results and light Higgs bosons in the 2HDM(II)*, *Acta Phys. Polon.* **B33** (2002) 2621 [hep-ph/0208076].

[22] Heavy Flavour Averaging Group, online at www.slac.stanford.edu/xorg/hfag.

[23] Belle collaboration, K. Abe et al., *A measurement of the branching fraction for the inclusive $B \to X/s\gamma$ decays with Belle*, *Phys. Lett.* **B 511** (2001) 151 [hep-ex/0103042];
Belle collaboration, P. Koppenburg et al., *An inclusive measurement of the photon energy spectrum in $b \to s\gamma$ decays*, *Phys. Rev. Lett.* **93** (2004) 061803 [hep-ex/0403004].

[24] CLEO collaboration, D. Cronin-Hennessy et al., *Hadronic mass moments in inclusive semileptonic B meson decays*, *Phys. Rev. Lett.* **87** (2001) 251808 [hep-ex/0108033].

JHEP04(2008)099

[25] BABAR collaboration, B. Aubert et al., *Measurements of the $B \to X_s\gamma$ branching fraction and photon spectrum from a sum of exclusive final states*, *Phys. Rev.* **D 72** (2005) 052004 [hep-ex/0508004]; *Measurement of the branching fraction and photon energy moments of $B \to X/s\gamma$ and $A(CP)(B \to X(s+d)\gamma)$*, *Phys. Rev. Lett.* **97** (2006) 171803 [hep-ex/0607071].

[26] A.J. Buras and M. Misiak, *$\bar{B} \to X/s\gamma$ after completion of the NLO QCD calculations*, *Acta Phys. Polon.* **B33** (2002) 2597 [hep-ph/0207131];
T. Hurth, *Present status of inclusive rare B decays*, *Rev. Mod. Phys.* **75** (2003) 1159 [hep-ph/0212304].

[27] M. Misiak et al., *The first estimate of $B(\bar{B} \to X/s\gamma)$ at $O(\alpha_s^2)$*, *Phys. Rev. Lett.* **98** (2007) 022002 [hep-ph/0609232].

[28] WMAP collaboration, D.N. Spergel et al., *Wilkinson Microwave Anisotropy Probe (WMAP) three year results: implications for cosmology*, *Astrophys. J. Suppl.* **170** (2007) 377 [astro-ph/0603449].

[29] B.C. Allanach, S. Kraml and W. Porod, *Theoretical uncertainties in sparticle mass predictions from computational tools*, *JHEP* **03** (2003) 016 [hep-ph/0302102].

[30] G. Bélanger, S. Kraml and A. Pukhov, *Comparison of SUSY spectrum calculations and impact on the relic density constraints from WMAP*, *Phys. Rev.* **D 72** (2005) 015003 [hep-ph/0502079].

JHEP04(2008)099